



## Cytoplasmic aggregation of DDX1 in developing embryos: Early embryonic lethality associated with *Ddx1* knockout

Matthew R. Hildebrandt<sup>1,2</sup>, Yixiong Wang<sup>1</sup>, Lei Li, Lubna Yasmin, Darryl D. Glubrecht,  
Roseline Godbout\*

*Department of Oncology, Cross Cancer Institute, University of Alberta, Edmonton, Alberta, T6G 1Z2, Canada*



### ARTICLE INFO

**Keywords:**  
DEAD box protein  
DEAD box 1  
Gene knock-out  
Embryonic development  
Maternal RNA  
RNA immunoprecipitation  
TIA-1

### ABSTRACT

Temporally-regulated maternal RNA translation is essential for embryonic development, with defective degradation resulting in stalled 2-cell embryos. We show that DDX1, a DEAD box protein implicated in RNA transport, may be a key regulator of maternal RNA utilization. DDX1 protein localizes exclusively to cytoplasmic granules in both oocytes and early stage mouse embryos, with DDX1 requiring RNA for retention at these sites. Homozygous knockout of *Ddx1* causes stalling of mouse embryos at the 2–4 cell stages. These results suggest a maternal RNA-dependent role for DDX1 in the progression of embryos past the 2–4 cell stage. The change in appearance of DDX1-containing granules in developing embryos further supports a role in temporally-regulated degradation of RNAs. We carried out RNA-immunoprecipitations (RNA-IPs) to identify mRNAs bound to DDX1 in 2-cell embryos, focusing on 16 maternal genes previously shown to be essential for embryonic development past the 1- to 2-cell stages. Five of these RNAs were preferentially bound by DDX1: Ago2, Zar1, Tle6, Floped and Tif1α. We propose that DDX1 controls access to subsets of key maternal RNAs required for early embryonic development.

### 1. Introduction

DEAD box 1 (DDX1) is an RNA helicase involved in cellular processes ranging from RNA transport to the repair of DNA double-strand breaks (Chen et al., 2002; Kanai et al., 2004; Li et al., 2017; Lin et al., 2014; Perez-Gonzalez et al., 2014; Popow et al., 2014; Ribeiro de Almeida et al., 2018; Robertson-Anderson et al., 2011). DDX1 is most often found in the nucleus of the cell where it associates with nuclear bodies involved in RNA processing such as Cajal bodies, gems and cleavage bodies (Bleoo et al., 2001; Li et al., 2006). DDX1 is also found in RNA granules located in the cytoplasm of neurons (Kanai et al., 2004; Miller et al., 2009). These RNA granules are involved in the transport of RNAs in neuronal cell bodies and processes so that they can be translated where they are needed. When cells are treated with ionizing radiation, DDX1 co-localizes with proteins involved in the repair of DNA double-strand breaks (Li et al., 2008b, 2016, 2017). There is evidence pointing to a role for DDX1 in the clearance of RNA at DNA double-strand breaks located in transcriptionally active genomic regions (Li et al., 2008b, 2016, 2017).

The biological role of DDX1 remains poorly understood. *DDX1* cDNA was first cloned from retinoblastoma cell lines carrying amplified copies of the *DDX1* and *MYCN* genes (Godbout and Squire, 1993). DDX1 was subsequently found to also be amplified and overexpressed in other pediatric cancers such as neuroblastoma and alveolar rhabdomyosarcoma (Akiyama et al., 1999; Amler et al., 1996; Godbout et al., 1998; Noguchi et al., 1996; Squire et al., 1995). More recently, elevated levels of cytoplasmic DDX1 have been shown to correlate with early recurrence in breast cancer, regardless of cancer subtype (Germain et al., 2011). Intriguingly, levels of DDX1 may be predictive of breast cancer response to chemotherapy and hormone therapy (Balko and Arteaga, 2011; Germain et al., 2011).

*Ddx1* knock-out models have been generated in both *Mus musculus* and *Drosophila melanogaster*. Although viable, *Ddx1*-null flies are smaller in size than their wild-type counterparts. Males are sterile due to disrupted spermatogenesis, whereas females show much reduced fertility with egg chambers undergoing autophagy (Germain et al., 2015). In contrast, loss of *Ddx1* function in mice leads to early embryonic lethality,

\* Corresponding author.

E-mail addresses: matthew.hildebrandt@sickkids.ca (M.R. Hildebrandt), yixiong@ualberta.ca (Y. Wang), leil@ualberta.ca (L. Li), lyasmin@ualberta.ca (L. Yasmin), darryl.glubrecht@albertahealthservices.ca (D.D. Glubrecht), rgodbout@ualberta.ca (R. Godbout).

<sup>1</sup> These authors contributed equally to the manuscript.

<sup>2</sup> Matthew R. Hildebrandt present address: Department of Molecular Genetics, The Hospital for Sick Children, Toronto, Ontario, M5G 0A4 Canada.

with embryos dying pre-blastocyst (Hildebrandt et al., 2015). This difference in phenotype between mice and flies may in part be explained by the presence of maternal Ddx1 protein in *Ddx1*-null flies up to the second instar, at 48 h post-egg laying (Germain et al., 2015). Intriguingly, we also observe *Ddx1* wild-type lethality when crossing second generation *Ddx1* heterozygote mice (Hildebrandt et al., 2015). Our results suggest that transcription of the wild-type *Ddx1* allele is up-regulated in *Ddx1*<sup>+/−</sup> mice, leading to lethality when these heterozygote mice are subsequently mated due to overexpression of DDX1 in wild-type mice.

The initial stages of mouse development are dependent on the maternal complement of transcripts and proteins (Li et al., 2010; Tang et al., 2007). In mammals, oocytes and surrounding cumulus cells generate the maternal transcripts required by the oocyte and the fertilized zygote. Maternally transcribed genes such as Zygote arrest 1 (*Zar1*) and transcription intermediary factor 1, alpha (*Tif1α* also known as *Trim24*) are important for the progression of the embryo beyond the 1- or 2-cell stage, respectively (Jiao and Woodruff, 2013; Torres-Padilla and Zernicka-Goetz, 2006; Wu et al., 2003). *Zar1* and *Tif1α* affect pronuclear syngamy and promote the first wave of zygotic genome activation, respectively.

For development to proceed past the initial divisions, the zygote has to undergo genome activation (Nothias et al., 1996; Schultz, 1993; Zeng and Schultz, 2005). The maternal-to-zygotic transition (MZT) occurs just after fertilization and is mostly completed by the 2-cell stage in mice and by the 8-cell stage in humans and bovines (Schultz, 1993, 2002; Telford et al., 1990). The first component of MZT is the active degradation of oocyte-specific transcripts, a process believed to trigger embryonic transcription (Piko and Clegg, 1982; Schultz, 2002). Transcript degradation in the cytoplasm is associated with the 'RNA induced silencing complex' (RISC) (Lykke-Andersen et al., 2008). The endoribonuclease Argonaute 2 (Ago2) encoded by maternal mRNA is one of the key proteins involved in the degradation of maternal transcripts and the loss of

the maternal Ago2 transcripts results in embryonic lethality at the 2-cell stage (Lykke-Andersen et al., 2008). Once oocyte-specific degradation occurs, embryonic genes are reprogrammed through chromatin remodeling and embryonic transcription activated (Clapier and Cairns, 2009; McLay and Clarke, 2003). The large burst of transcription associated with zygotic gene activation does not occur until the 2-cell stage, and there is no delay in the translation of these transcripts (Carter et al., 2003; Hamatani et al., 2004; Wang et al., 2004).

We have previously shown that *Ddx1*<sup>−/−</sup> mouse embryos die prior to the blastocyst stage (Hildebrandt et al., 2015). Here, we demonstrate that *Ddx1*<sup>−/−</sup> embryonic development stalls at the 2- to 4-cell stages *in vitro*. Based on immunostaining data, DDX1 is predominantly found in cytoplasmic granules in pre-implantation embryos. Cytoplasmic DDX1 granules are dynamic, changing in size and appearance as development progresses from the zygote to the blastocyst stages. DDX1 granules co-localize with two proteins previously associated with stress granules, TIA-1 and TIAR (Kedersha et al., 1999). Our data suggest that DDX1, but not TIAR/TIA-1, accumulation in cytoplasmic granules in early embryos is dependent on the presence of RNA. We propose that DDX1 is part of an essential complex that controls RNA bioavailability early in embryonic development by binding to maternal transcripts that are essential for early embryonic development.

## 2. Results

### 2.1. DDX1 expression in adult mouse ovaries and maturing oocytes

We examined the subcellular localization of DDX1 in mouse ovaries. DDX1 was highly expressed in the developing oocytes and the surrounding granulosa cells of the ovaries (Fig. 1A). Stromal cells between follicles had low to no expression of DDX1, while the cells of the corpus luteum were positive for nuclear DDX1 with weak diffuse cytoplasmic

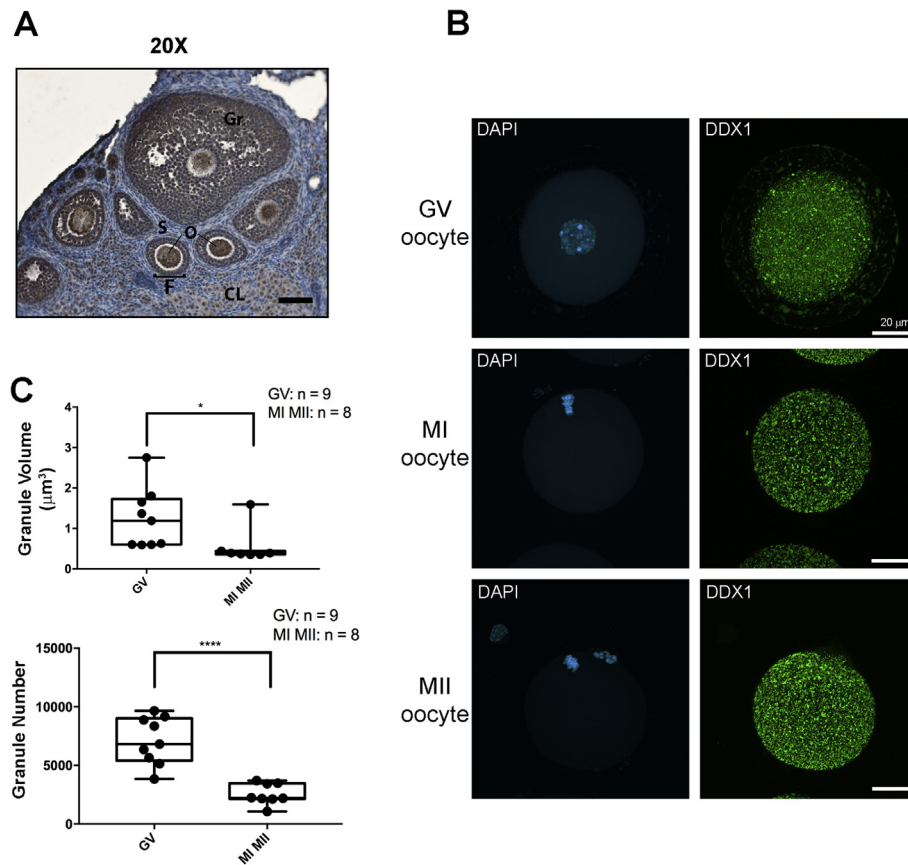


**Fig. 1. DDX1 expression in mouse ovaries and oocytes.** (A) Sections of adult mouse ovaries were immunostained with anti-DDX1 antibody. Gr: Granulosa cells; O: Oocytes; F: Follicles; S: Stromal cells; CL: Corpus luteum. (B) Germinal vesicle oocytes, MI (meiosis I) oocytes and MII oocytes were immunostained with anti-DDX1 antibody and counterstained with DAPI for nucleus detection. Oocytes are displayed as 2D projections of Z-stacks imaged by confocal microscopy. Scale bars = 20  $\mu$ m. (C) Surface rendering by Imaris software was used to calculate the number and volume of DDX1 granules. Statistical differences were calculated by Welch's *t*-test using Prism software (\* $P < 0.05$ ; \*\*\* $P < 0.0001$ ).

staining. All oocytes examined, regardless of maturation state, showed a strong DDX1 signal throughout the cytoplasm.

To further examine the subcellular distribution of DDX1 in oocytes, we collected oocytes at the germinal vesicle (GV) stage (immature oocytes) from both C57BL/6 and FVB mice. GV oocytes were immunostained with anti-DDX1 antibody and z-stacks were used to generate maximum intensity projections of DDX1 localization. Imaris software was used to reconstruct 3D structures from the z-stacks. DDX1 granules averaging  $1.2 \mu\text{m}^3$  in volume were found throughout the cytoplasm with  $\sim 7000$  granules per GV oocyte (Fig. 1B and C). No DDX1 was detected in the nucleus based on examination of single optical sections. Similar results were obtained in meiosis I (MI) and meiosis II (MII) oocytes, except that there were fewer DDX1 granules per oocyte and DDX1 granules were smaller in size (Fig. 1B and C).

## 2.2. DDX1 expression in pre-implantation embryos

Analysis of single-cell RNA sequencing data (Biase et al., 2014) revealed significant increases in *Ddx1* RNA levels from the zygote to the 4-cell stage, with an  $\sim 2$ -fold increase from zygote to 2-cell stage, and a further 3-fold increase from the 2-cell to 4-cell stage (Fig. 2). These results suggest that *Ddx1* is one of the few zygotic genes activated during the minor wave of the MZT starting at zygote stage. We therefore examined DDX1 distribution in early stage embryos. In 1-cell stage embryos, the DDX1 immunostaining pattern was similar to that observed in unfertilized oocytes, with numerous granules found throughout the cytoplasm of the embryo (Fig. 3A). There was no detectable DDX1 in the nucleus of 1-cell stage embryos. DDX1 remained abundant in 2-cell and 4-cell embryos, with numerous DDX1-containing granules observed throughout the cytoplasm. By the 4-cell stage, fewer DDX1 granules were present; however, they appeared larger and less circular. By the 8-cell stage, DDX1 granules were variable in size and shape with what appeared to be aggregates (or clumps) of DDX1 granules throughout the cytoplasm. This trend towards aggregation was even more obvious in blastocysts, with fewer, but larger granules observed. Aggregates were unevenly distributed in blastocyst cells, and were mostly found surrounding the nucleus.

We quantified the gradual decrease in the number of DDX1 granules from the 1-cell (zygote) stage to the blastocyst stage (Fig. 3B and C). In 1-cell embryos, there was an average of  $\sim 3200$  granules per embryo and the average granule size was  $0.9 \mu\text{m}^3$ . In 2-cell embryos, there was an average of  $\sim 1700$  granules with an average volume of  $2.6 \mu\text{m}^3$ . In 4-cell stage embryos, there were  $\sim 600$  DDX1 granules per embryo with an

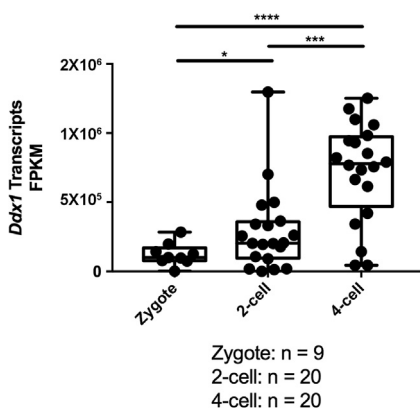


**Fig. 2. *Ddx1* RNA in embryos.** Single cell sequencing data for zygotes, 2-cell and 4-cell stage embryos were obtained from Biase et al. (Biase et al., 2014). Data were merged with custom R scripts and rssqlite package. DDX1 expression profiles were extracted and plotted with Prism. Unpaired t-test between 2- and 4-cell embryos, Welch's t-test between zygote and 2-cell, and Welch's t-test between zygote and 4-cell were performed with Prism (\* $P < 0.05$ ; \*\* $P < 0.001$ ; \*\*\* $P < 0.0001$ ).

average volume of  $\sim 9 \mu\text{m}^3$ . There was one outlier with elevated granule numbers in the 4-cell embryo sample group, but this may have been an early 4-cell embryo in which the smaller DDX1 granules were still transitioning to larger granules. By the 8-cell stage, DDX1 granules had again increased in size to  $\sim 12 \mu\text{m}^3$  although there was significant variation in granule volume. There were only  $\sim 200$  large granules per 8-cell embryo. Large DDX1 aggregates with variable appearance were observed at the early (32-cell) blastocyst stage. While the total number of distinct aggregates was low ( $\sim 50$ ), these varied in volume from  $15$  to  $60 \mu\text{m}^3$ . There was no significant difference in either the numbers or appearance of DDX1 aggregates in the inner cell mass (ICM) and trophoblast cells of early blastocysts.

As mentioned earlier, DDX1 is primarily found in the nucleus of post-embryonic cells. To determine when the transition from a primarily cytoplasmic localization to a primarily nuclear localization takes place during development, we immunostained later stage blastocysts cultured from 1-cell embryos. A reduction in cytoplasmic DDX1, accompanied by an increase in nuclear DDX1, was observed as blastocysts transitioned from early (Fig. 3A, bottom panels) to late stages (Fig. 4A). DDX1 subcellular distribution was similar in the ICM and trophoblast cells of later stage embryos (magnified in Fig. 4A). To examine DDX1 subcellular distribution in hatched blastocysts, we cultured E3.5 blastocysts for 48 and 72 h. Hatched blastocysts at 48 h showed weak DDX1 immunostaining in the nucleus of trophoblast cells (Fig. 4B). By 72 h in culture, the majority of DDX1 was found in the nucleus of trophoblast cells (Fig. 4B). The thickness of the ICM in hatched embryos precluded detailed analysis of DDX1 subcellular distribution. Overall, these results suggest different roles for DDX1 in embryos compared to post-embryonic tissues.

To determine whether there are different forms of DDX1 in embryos versus post-embryonic cells, we first examined single-cell RNA sequencing data (GSE57249) from 1-cell, 2-cell, 4-cell, 8-cell and blastocyst embryos (Biase et al., 2014). All exons were present in these early stage embryos (data not shown). Although 90% of the single cell sequencing data from 2-cell and 4-cell stages showed identical *DDX1* RNA sequencing patterns to that of post-embryonic RNA, we noted that a small percentage of 2-cell and 4-cell stage embryos (4/40 embryos), but not ICM or trophoblast cells (0/7), had sequences that mapped to intron 1. To pursue the possibility of alternative splicing in early stage embryos, we extracted RNA from 2 sets of 2-cell stage embryos and used RT-PCR and four sets of primers spanning all known exons of *Ddx1* to examine embryonic *Ddx1* RNA. Although the signal intensity was weak using primers spanning exons 1 and 9, bands were of the expected sizes and appeared identical to bands obtained using adult mouse brain RNA (Fig. 5A). Similarly, primers designed to amplify exons 10 to 16, exons 17 to 21 and exons 22 to 26 generated same size bands using 2-cell and adult mouse brain RNA.

To further investigate the possibility of different forms of DDX1 being expressed in early stage embryos versus post-embryonic cells, we carried out western blotting using lysates prepared from two hundred 2-cell stage embryos, R1 mouse embryonic stem cells (E3.5), and adult mouse brain. Similar size DDX1 protein bands were observed in all three samples using two different anti-DDX1 antibodies recognizing the N-terminus (aa 1–186) or C-terminus (aa 187–740) of DDX1 (Fig. 5B and C). Thus, based on combined RNA sequencing, RT-PCR and Western blot analyses, we were unable to find evidence of different forms of DDX1 in early stage embryos versus post-embryonic cells.

## 2.3. DDX1 granules do not co-localize with proteins associated with RNA decay and RNA processing bodies

As DEAD box proteins are known to be involved in RNA transport, RNA processing and RNA degradation, we co-immunostained 2-cell embryos using antibodies that detect proteins associated with various RNA-related processes: DDX3 (Fig. 6; with magnification in Fig. S1), involved in RNA transport and translational control, and associated with

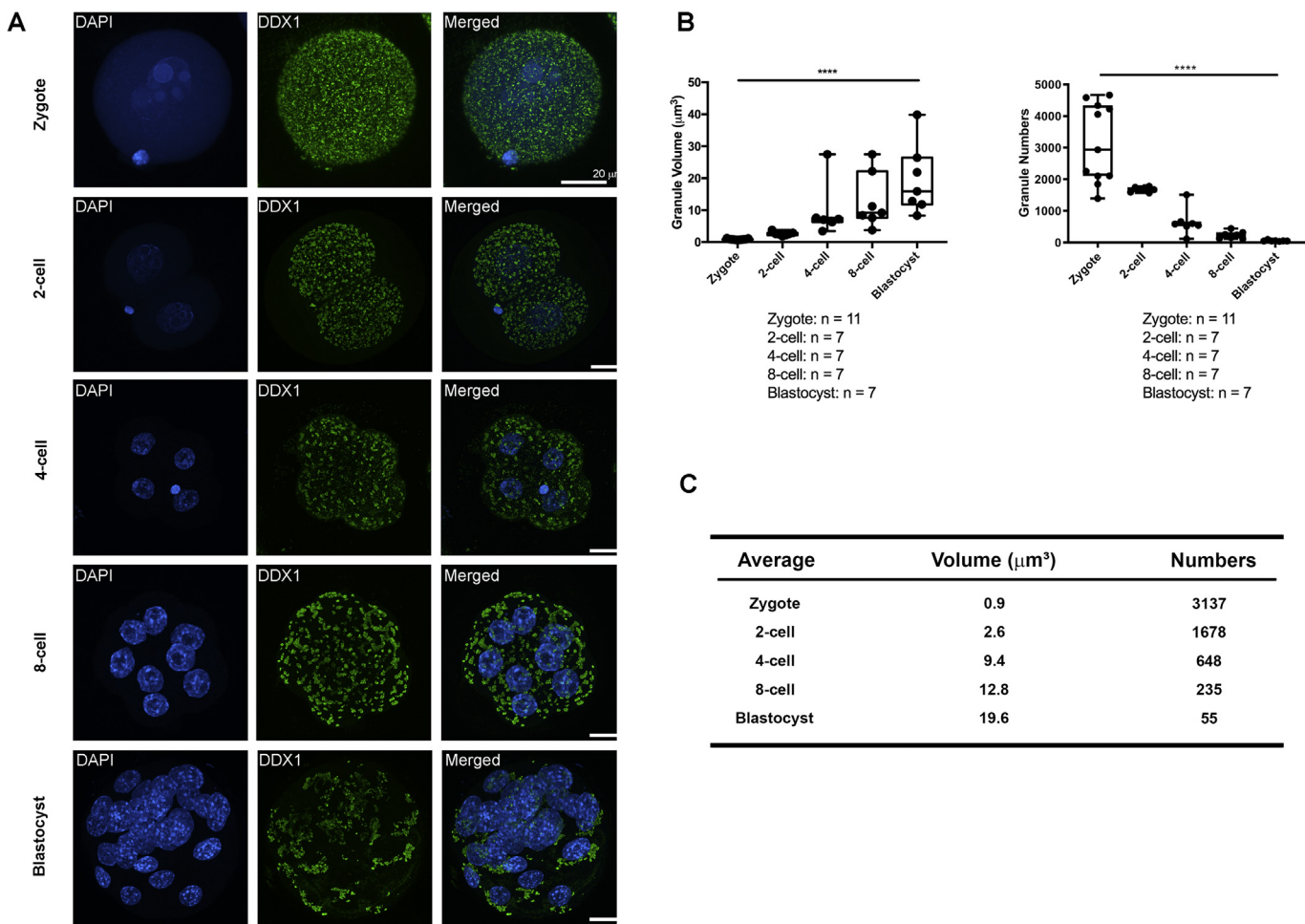


**Fig. 3. DDX1 localization in pre-implantation embryos.** (A) Embryos at stages E0.5 (zygote or 1-cell), 1.5 (2-cell), 2 (4-cell), 2.5 (8-cell) and 3.5 (blastocyst) were immunostained with anti-DDX1 antibody and counterstained with DAPI for nucleus detection. DDX1 granules were observed exclusively in the cytoplasm. Embryos are displayed as 2D projections of Z-stacks imaged by confocal microscopy. Scale bars = 20  $\mu\text{m}$ . (B, C) Surface rendering by Imaris software was used to calculate the number (B) and volume (C) of DDX1 granules at each embryonic stage. Statistical differences were calculated by one-way ANOVA using Prism software. (\*\*\*\* indicates  $P < 0.0001$ ).

processing (P)-bodies (Chahar et al., 2013; Lai et al., 2008; Soto-Rifo et al., 2012); EXOSC5 (Fig. 6; with magnification in Fig. S2), a component of the exosome associated with RNA processing and degradation (Mae-kawa et al., 2015; Zinder and Lima, 2017); GW182 (Fig. 6; with magnification in Fig. S3), associated with miRNA silencing and GW-bodies or P-bodies (Serman et al., 2007); and p54/RCK (DDX6) (Fig. 6; with magnification in Fig. S4), associated with P-bodies (Ayache et al., 2015; Chahar et al., 2013; Tritschler et al., 2009). There was no co-localization of DDX1 granules with any of these proteins. Similarities in the localization of DDX3, GW182 and DDX6 suggest focused RNA processing/degradation activity at opposite poles near the outer edge of 2-cell embryos. We also examined whether DDX1 was associated with either mitochondria or endoplasmic reticulum (ER). No co-localization was observed between DDX1 granules and either MitoTracker Deep Red, a mitochondria staining dye (Fig. S5) or calnexin, an ER marker (Fig. S6).

#### 2.4. DDX1 granules co-localize with TIA-1 and TIAR, proteins normally found in stress granules of somatic cells

DDX1 aggregates in nuclear bodies of mammalian (non-embryonic) cell lines cultured under normal growth conditions. Exposure to stressors such as heat shock and oxidative stress results in aggregation of DDX1 in cytoplasmic stress granules (Kunde et al., 2011; Onishi et al., 2008). We therefore co-immunostained early stage embryos with anti-DDX1

antibody as well as antibodies to stress granule markers including TIA-1 and TIAR (Kedersha et al., 1999). Co-localization of TIA-1 with DDX1 granules was not observed in 1-cell stage embryos; however, significant co-localization was observed from the 2-cell to blastocyst stages (Fig. 7). Co-immunostaining of TIAR with DDX1 granules was also observed in embryos, but only from late 2-cell to 8-cell stages (Fig. S7). In contrast to DDX1 and TIA-1, TIAR expression was restricted to the nucleus at the blastocyst stage. We also examined co-localization of SMN with DDX1 granules, as DDX1 nuclear bodies reside adjacent to or co-localize with gems (SMN-containing nuclear bodies) (Bleoo et al., 2001; Li et al., 2006), and SMN is observed in stress granules when mammalian cells are exposed to stress-inducing agents. There was no clear co-localization of SMN with DDX1 granules in 2-cell stage embryos (Fig. S8). Similarly, co-immunofluorescence analysis using two other markers of stress granules, FXR1 and RACK1 (Arimoto et al., 2008; Gareau et al., 2013; Herman et al., 2018; Mazroui et al., 2002; Ohn et al., 2008), showed no co-localization with DDX1 granules (Fig. S9). These results suggest that co-localization of TIA-1 and TIAR with DDX1 granules does not simply represent a reconstruction of stress granule-like structures in embryos but reflects an embryo-specific association between DDX1 granules and TIA-1/TIAR proteins.

As TIA-1 and TIAR are both associated with stress granules in mammalian cell lines, we were interested to see if the number and appearance of DDX1 granules were affected by stress. Embryos were collected and either heat-shocked at 43 °C for 45 min or incubated at

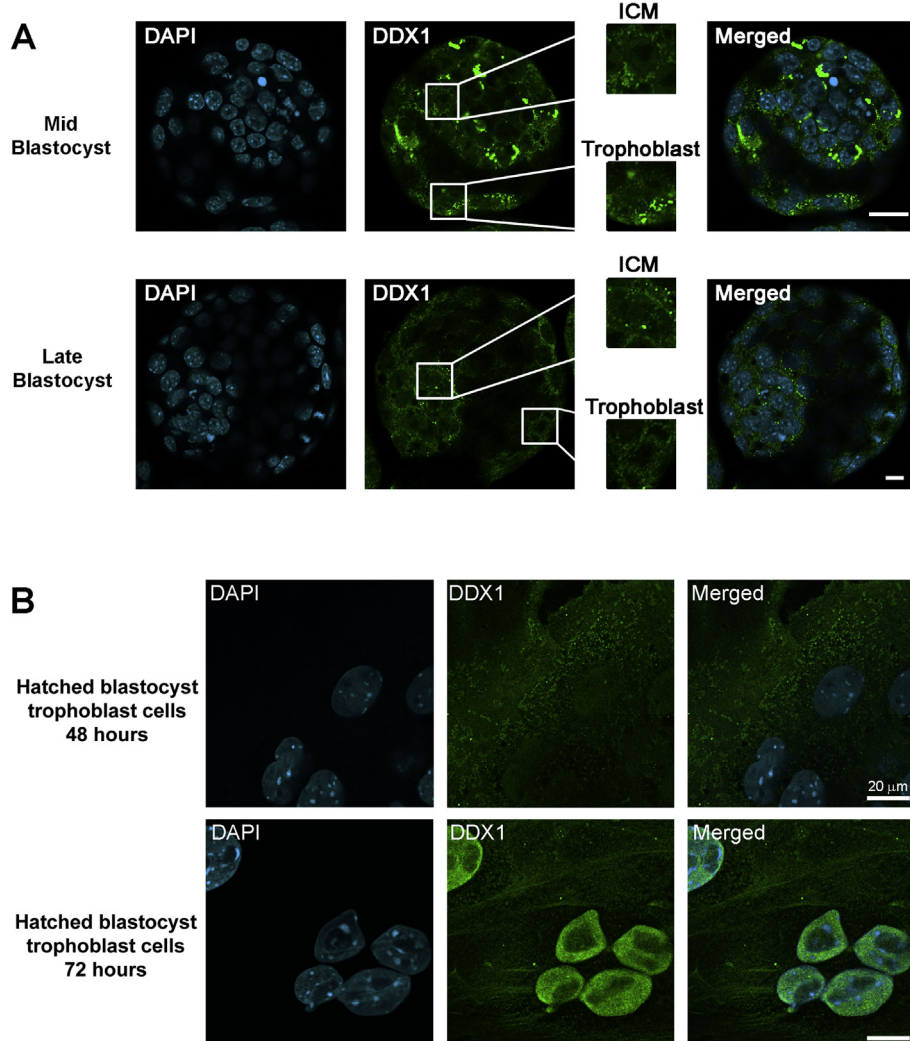


**Fig. 4. DDX1 relocates to the nucleus in late blastocysts.** (A) 1-cell stage embryos were cultured in M16 medium to the blastocyst stage. Mid and late pre-hatched blastocyst stages were selected based on blastocyst size and cell numbers, and immunostained with anti-DDX1 antibody. Cytoplasmic DDX1 granules gradually disappeared with blastocyst development. The DDX1 signal is purposely saturated to more clearly show the presence of DDX1 in the nucleus. A magnification of the inner cell mass (ICM) and trophoblast cells is shown on the right. (B) E3.5 embryos were cultured for either 48 h or 72 h and hatched blastocysts immunostained with anti-DDX1 antibody. DAPI was used to stain the nuclei. An increase in the relative amount of DDX1 in the nucleus of trophoblasts in hatched blastocysts was observed at 48 h compared to pre-hatched blastocysts. By 72 h, most of the DDX1 was found in the nucleus of trophoblasts. The ICM of hatched blastocysts was too thick to allow accurate visualization of DDX1 subcellular patterns. Scale bars = 20  $\mu$ m.

37 °C in KMSO medium for 45 min. Embryos were then fixed and immunostained with anti-DDX1 and either anti-TIA-1 or TIAR antibodies. There was no difference between control and heat-shocked embryos in either the immunostaining patterns of DDX1 and TIA-1 or that of DDX1 and TIAR (Fig. S10). Similar results were observed when we treated 2-cell embryos with 1 mM H<sub>2</sub>O<sub>2</sub> for 4 h (data not shown). These results suggest that early stage embryos do not form classic-style stress granules in response to environmental stress.

#### 2.5. DDX1 granule formation is dependent on RNA and transcription but not translation

We next asked whether RNA is required for DDX1 granule formation in early embryos. We first stained 2-cell stage embryos with acridine orange (2  $\mu$ M for 20 min) to see if acridine orange could be used to detect RNAs in DDX1 granules. Although numerous small foci, along with a few large foci, were observed in acridine orange-stained cells, there was no apparent co-localization of acridine orange with DDX1 granules (Fig. 8A). One possibility is that acridine orange is not able to access the RNAs bound by DDX1.

As a second approach, we treated 2-cell stage embryos with ribonuclease A (RNase A) to examine the effect of RNA removal on the number and appearance of DDX1 granules. Embryos were pre-treated with 0.1% saponin prior to fixation followed by treatment with 150  $\mu$ g/ml RNase A in PBS. Saponin-treated embryos followed by incubation in PBS served as the negative control. Embryos were then fixed, co-immunostained with

anti-DDX1 and anti-TIA-1 antibody, and imaged. Although detergent treatment caused some cell shrinkage, DDX1/TIA-1 granules were still present in control embryos (Fig. 8B). However, upon RNase A treatment, a significant portion of DDX1 granules disappeared resulting in mostly diffuse cytoplasmic DDX1 immunostaining. Intriguingly, TIA-1 localization to granules was unaffected by RNase A treatment (Fig. 8B). These data suggest that DDX1 forms a complex with RNA during early embryonic stages, and that RNA is required for retention of DDX1, but not TIA-1, within granules.

We then examined the effect of transcription and translation inhibitors on DDX1 granules. Treatment of 2-cell stage embryos with 100  $\mu$ g/ml cycloheximide for 8 h (to inhibit translation) had no effect on either the number or appearance of DDX1 granules (Fig. 9A). However, treatment of 2-cell stage embryos with 200  $\mu$ M cordycepin for 8 h (to inhibit transcription) resulted in some disruption/clumping of DDX1 granules (Fig. 9B). These results suggest a role for newly-synthesized RNA but not newly-synthesized protein in maintenance of the DDX1 granules typically observed in 2-cell stage embryos.

#### 2.6. *Ddx1*<sup>-/-</sup> embryos stall at the 2- to 4-cell stage

Genotyping analysis revealed loss of *Ddx1*<sup>-/-</sup> embryo prior to the blastocyst stage. To further address when *Ddx1*<sup>-/-</sup> embryos die, E0.5 embryos from either wild-type or first generation *Ddx1*<sup>+/-</sup> X *Ddx1*<sup>+/+</sup> intercrosses were collected and allowed to develop *in vitro* in microdroplets of KMSO culture medium. The embryos were examined for their

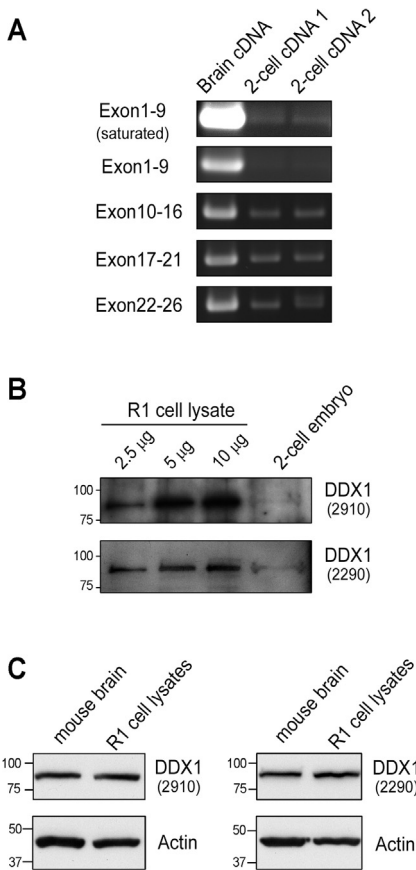


**Fig. 5. DDX1 RNA and protein in 2-cell embryos, R1 cells and mouse brain.** (A) Total RNAs were prepared from either seven or eight 2-cell embryos (obtained from two mice), or adult mouse brain tissue. RT-PCR analysis was carried out using 4 sets of primers covering all *Ddx1* exons. The signal obtained for exons 1 to 9 was saturated in order to visualize the bands in 2-cell embryos. (B) Whole cell lysates were prepared from 2-cell embryos and R1 cells. Different amounts of R1 cell lysate (2.5 µg, 5 µg and 10 µg per lane) were loaded to allow comparison with 2-cell embryos. (C) Forty µg whole cell lysates from either adult mouse brain or R1 cells were loaded in each lane. (B, C) Cell lysates were electrophoresed in SDS-PAGE gels and immunoblotted using two different anti-DDX1 antibodies targeting different parts of DDX1 [N-terminal DDX1 (aa 1–186) and C-terminal DDX1 (aa 187–740)]. Size markers are indicated on the left of each blot.

developmental progression every 24 h. For wild-type crosses, we found the expected progression from 2- to 4- to 8-cell stages at 24 h, 48 h and 72 h, respectively. Of the 17 wild-type embryos analysed, 94% (16/17) reached the 8-cell stage by 72 h, with one embryo stalled at the 1-cell stage for the duration of the experiment (Table 1). For heterozygous intercrosses, 92% (134/146) of the embryos reached 2-cell stage by 24 h. However, only 99 embryos (68%) and 94 embryos (64%) reached 4- and 8-cell stages by 48 h and 72 h, respectively (Table 1). Thirty-five embryos (24%) were still at the 2-cell stage at 48 h, while 24 embryos (16%) and 16 embryos (11%) were at the 2-cell and 4-cell stage, respectively, at 72 h. Thus, 16% of intercross embryos failed to progress past the 2-cell stage, and an additional 11% failed to progress past the 4-cell stage after 72 h. Twelve embryos (8%) remained at the one-cell stage throughout the time analysed. In comparison, 1/17 (5%) of wild-type embryos remained at the one-cell stage.

To determine whether the stalled embryos were *Ddx1*<sup>-/-</sup>, we cultured embryos from both wild-type and first generation *Ddx1*<sup>+/−</sup> intercrosses for 72 h, fixed and immunostained the embryos with anti-DDX1 antibody. 2- and 4-cell stage embryos from wild-type crosses showed abundant DDX1 granules throughout the cytoplasm (Fig. 10A). In contrast, stalled 2-cell and 4-cell stage embryos from *Ddx1*<sup>+/−</sup>

intercrosses had an abnormal number of nuclei and virtually no DDX1 immunostaining (Fig. 10B).

### 2.7. DDX1 RNA-immunoprecipitation of 2-cell stage embryos

Like other members of the DEAD box family, DDX1 binds RNA (Chen et al., 2002; Han et al., 2014; Li et al., 2008b, 2016). To address DDX1's role in embryonic development, we carried out RNA-DDX1 immunoprecipitation to identify RNAs bound to DDX1. We collected three hundred 2-cell stage embryos and divided them into 2 groups: control immunoprecipitation with IgG and experimental immunoprecipitation with DDX1 antibody. To identify potential RNA targets of DDX1, we carried out RT-qPCR of 16 genes whose maternal absence causes stalling of embryo development at 1- to 2- or 2- to 4-cell stages. Included in our set of 16 genes were Ago2 (Lykke-Andersen et al., 2008), *Bnc1* (Ma et al., 2006), *Brg1* (Griffin et al., 2008; Singh et al., 2016), *Brwd1* (Pattabiraman et al., 2015; Philippis et al., 2008), *Dicer1* (Murchison et al., 2007; Tang et al., 2007), *Floped* (Li et al., 2008a), *Hr6α* (Roest et al., 2004), *Mater* (Tong et al., 2000), *Padi6* (Xu et al., 2016; Yurttas et al., 2008), *Tle6* (Li et al., 2008a), *Tif1α* (Torres-Padilla and Zernicka-Goetz, 2006), *Zar1* (Wu et al., 2003), *Filia* (Ohsugi et al., 2008), *Hsf1* (Bierkamp et al., 2010; Christians et al., 2000), *Npm2* (Kim and Lee, 2014; Ogushi et al., 2017), *Zfp36l2* (Li et al., 2010; Ramos et al., 2004).

Three independent pre-amplifications from each of the IgG and DDX1 immunoprecipitations were carried out to generate sufficient material for RT-qPCR analysis. Although a significant amount of variation was observed between the three technical replicates, 8/16 RNAs (*Ago2*, *Brwd1*, *Dicer1*, *Floped*, *Tle6*, *Tif1α*, *Zar1* and *Zfp36l2*) showed close to 10-fold increases compared to IgG control. Of these 8 RNAs, 2 RNAs (*Ago2* and *Zar1*) showed differences of 2-fold or higher in 2 pre-amplifications and 3 (*Tle6*, *Floped* and *Tif1α*) showed differences of 2-fold or higher in all 3 pre-amplifications (Fig. 11).

### 3. Discussion

DDX1 is widely expressed in cell lines and tissues, with a primarily nuclear distribution (Bleoo et al., 2001; Godbout et al., 2002, 2007). In general, proliferating cells and cells of neuroectodermal origin express the highest levels of DDX1 (Fagerberg et al., 2014). We observed differences in the localization of DDX1 within ovaries, with cortical stroma cells and granulosa cells in follicles showing both nuclear and cytoplasmic DDX1. Cells of the theca externa (cells directly surrounding the follicles) showed either low or no DDX1 expression. Oocytes within each follicle also had very high levels of DDX1, but in contrast to granulosa cells, DDX1 was exclusively found in the cytoplasm. The cytoplasmic distribution of DDX1 observed after fertilization (1-cell to blastocyst stages) suggests related roles for DDX1 in oocytes and early stage embryos.

The appearance of cytoplasmic DDX1 granules underwent a dramatic change over time. In oocytes and 1-cell embryos, DDX1 was found in small granules throughout the cytoplasm, in keeping with the reported uniform distribution of maternal RNAs in oocytes and early embryos (Xie et al., 2018). After fertilization, the number of DDX1 granules gradually decreased while increasing in size, seemingly aggregating with each other in blastocysts. As DDX1 granules are already present in maturing oocytes, and RNA is required for DDX1 aggregation in granules, an explanation for the changes in DDX1 distribution patterns is that DDX1's binding targets are maternal RNAs which are progressively getting degraded. It has been estimated that ~100 picograms of maternal RNAs are stored in developing oocytes (Clarke, 2012; Eckersley-Maslin et al., 2018; Piko and Clegg, 1982). These RNAs play key roles in embryonic development and undergo highly-regulated programs of translational activation and degradation. Mechanisms underlying their protection versus translation versus degradation remain poorly understood. We propose that DDX1 either protects or regulates the availability of maternal mRNAs during early embryonic development. As the need for

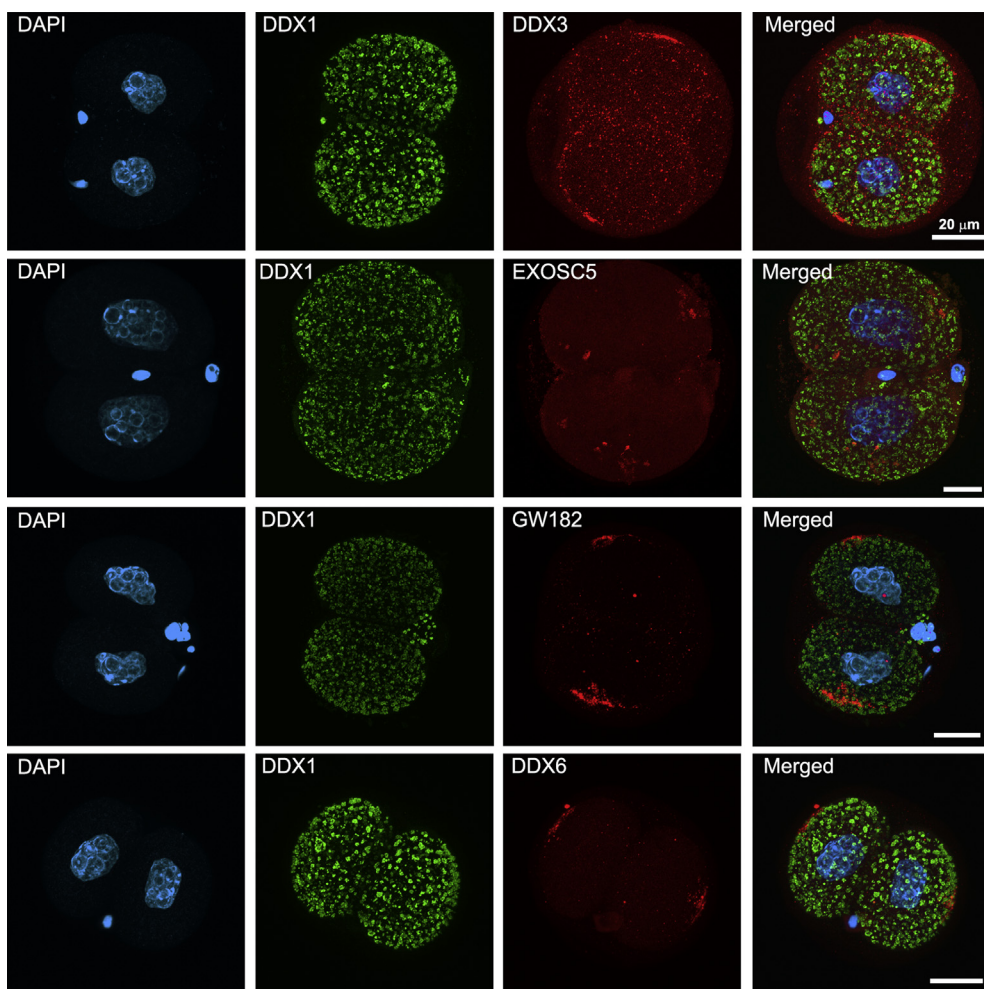


**Fig. 6. DDX1 does not co-localize with RNA processing bodies.** Two cell stage embryos were co-immunostained with DDX1 and the following antibodies: anti-DDX3 (P-bodies), anti-EXOSC5 (exosome), anti-GW182 (P-body), and anti-DDX6 (P-body). There was no co-immunostaining of DDX1 with any of these proteins. Embryos are displayed as 2D projections of Z-stacks imaged by confocal microscopy. Scale bar = 20  $\mu$ m.

maternal RNAs decreases and maternal RNAs are degraded, DDX1 binds to fewer RNAs resulting in larger aggregates as the result of clustering of DDX1 with the remaining maternal RNAs. In this regard, it is interesting that the localization of DDX1 granules within embryos changes over time, shifting from throughout the cytoplasm to large aggregates primarily located on one side of the nucleus. The latter may represent positioning of DDX1 for rapid entry into the nucleus once the proper signals are in place. In keeping with this idea, analysis of DDX1 subcellular localization in cultured blastocysts shows that DDX1 begins to move into the nucleus of ICM and trophoblast cells at the later blastocyst stages.

Development-dependent alterations in the subcellular localization of DDX1 could be driven by a number of factors, including alternative splicing giving rise to different DDX1 isoforms, post-translational modifications such as phosphorylation, as well as DDX1 protein interactors. To our knowledge, there are no reports of DDX1 alternative splicing in the literature although RNA sequencing databases reveal the presence of intronic regions in some cell types. Of specific relevance to our study, single cell sequencing of early stage mouse embryos (Biase et al., 2014) indicates the presence of DDX1 intron 1 sequences in a small percentage (~10%) of embryos. However, we were not able to confirm the presence of intron 1 sequences, or obtain evidence of alternative splicing, in 2-cell stage embryos based on RT-PCR. Similarly, there are a number of reports indicating that DDX1 can be phosphorylated (Han et al., 2014; Li et al., 2008b) as well as ubiquitinated (Oshikawa et al., 2012). Again, we were not able to obtain evidence of post-translational modification of 2-cell stage embryos based on western blotting. As not all post-translational

modifications cause a shift detectable by western blotting, additional strategies (e.g. 2D gel electrophoresis) will be required to further investigate the nature of DDX1 in early stage embryos compared to later-stage cells. Whether DDX1 is post-translationally modified or not in early stage embryos, it seems likely that protein interactors play a key role in the mobilization and subcellular localization of DDX1 during development.

DDX1 has previously been reported to associate with cytoplasmic RNA-containing granules, including RNA transport granules in neuronal cells and stress granules in mammalian cells exposed to environmental stressors such as heat shock (Kanai et al., 2004; Miller et al., 2009; Onishi et al., 2008). Although various RNA-binding protein (RNP) complexes have been described in early stage mouse embryos, including P-bodies (Chuma et al., 2006; Clark and Eddy, 1975; Flemr et al., 2010; Kim et al., 2012; Lue et al., 1999; Peplig et al., 2007; Spiegelman and Bennett, 1973; Voronina et al., 2011), DDX1 granules appear to be distinct from these as we observed no co-immunostaining of DDX1 with DDX3, GW182 or DDX6 (markers for P-bodies and germ cell granules). Intriguingly, we found co-localization of DDX1 granules with two RNA-binding proteins, TIA-1 and TIAR, normally associated with stress granules in mammalian cells exposed to environmental stressors such as heat-shock and oxidative stress (Arimoto-Matsuzaki et al., 2016; Gilks et al., 2004; Kedersha et al., 1999; McDonald et al., 2011). This association was found as early as 2-cell stage embryos.

Stress granules are sites of RNA triage, and contain messenger ribonucleoproteins stalled in translation initiation (Anderson and Kedersha, 2008; Proter and Parker, 2016). TIA-1 and TIAR play structural and

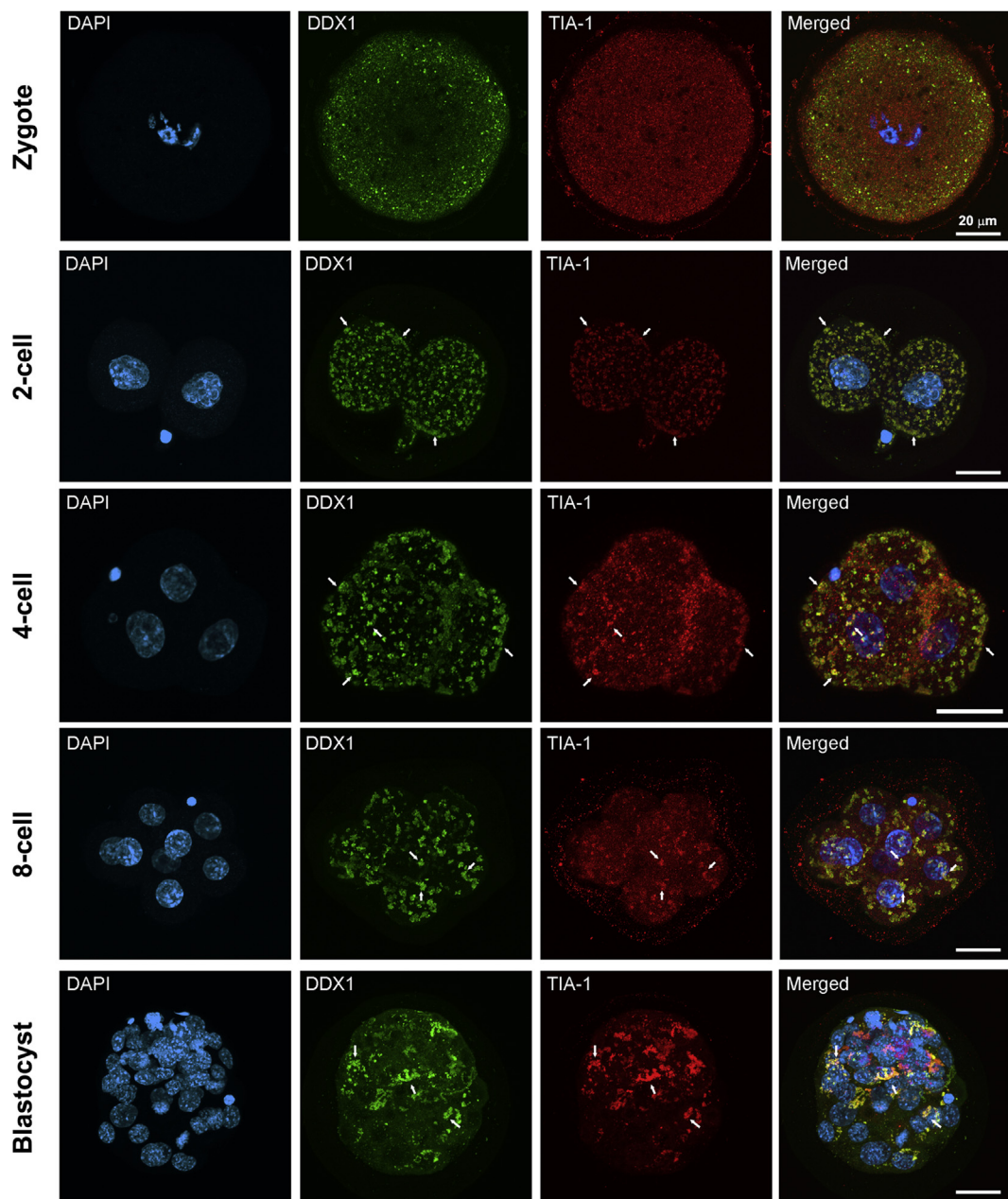


**Fig. 7. DDX1 co-localizes with TIA-1 in pre-implantation embryos.** DDX1 co-immunostaining with anti-TIA-1 antibody revealed co-localization of TIA-1 with DDX1 granules from the zygote to the blastocyst stages. Arrows point to DDX1 granules that co-localize with TIA-1. Embryos are displayed as 2D projections of Z-stacks imaged by confocal microscopy. Scale bar = 20  $\mu$ m.

functional roles in stress granules, acting as recruitment sites for other proteins as well as transcripts (Bley et al., 2015; Gilks et al., 2004; Kedersha et al., 1999). DDX1 and TIA-1 co-immunostaining was observed from the 2-cell to blastocyst stages, as well as in cultured blastocysts. In contrast, there was little co-immunostaining between DDX1 and TIAR by the 8-cell stage, with TIAR showing a primarily nuclear distribution pattern in 8-cell embryos and blastocysts. Unlike DDX1 granules which were affected by RNase A treatment, the distribution pattern of TIA-1 in granules did not change when 2-cell embryos were treated with RNase A. These results suggest that whereas RNA is required for the retention of DDX1 in granules, this is not the case for TIA-1. As TIA-1 has previously been associated with transport of RNAs to stress granules (Gilks et al., 2004), it's possible that TIA-1 is also involved in the transport of RNAs within the early stage embryos. Of note, none of the other components of stress granules tested, including FXR1 and RACK1

co-localized with DDX1 granules. Therefore, although they contain RNA, DDX1 granule formation in embryos may not be related to stress granule formation per se, but may co-opt components of stress granules for their specialized roles in embryos.

*Ddx1* knockout embryos die pre-blastocyst, whereas both *Tia-1* and *Tiar* knockout mice display lethality post-blastocyst, with some knockout mice surviving to adulthood with normal lifespans (Beck et al., 1998; Piecyk et al., 2000). Based on our embryo cultures, *Ddx1*<sup>-/-</sup> embryo die between the 2- and 4-cell stages. Our results thus suggest an essential cytoplasmic role for DDX1 in pre-implantation development, likely involving maternal RNAs. Upon fertilization, embryos must shift from reliance on maternal RNAs and protein to zygotic transcription and translation. One of the key processes in this transition is the controlled degradation of maternal RNAs (Li et al., 2010; Nothias et al., 1995; Schultz, 2002). The absence of certain maternal mRNAs such as *Zar1*,

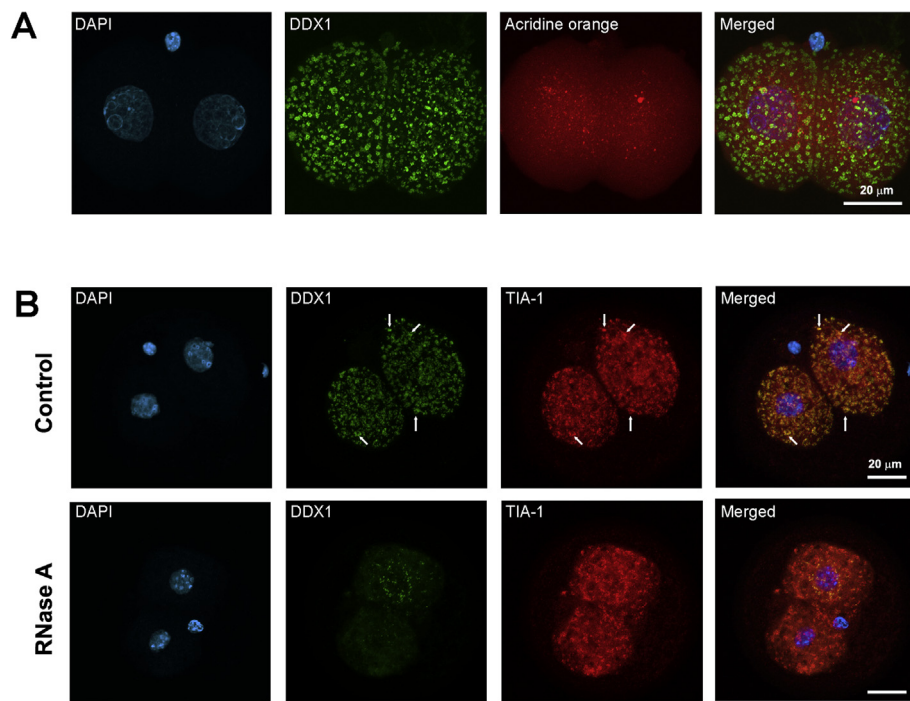


**Fig. 8.** DDX1 localization to DDX1 granules depends on the presence of RNA. (A) Embryos were incubated with 2 μM acridine orange for 20 min prior to immunostaining with DDX1 antibody. Immunofluorescence analysis revealed no clear pattern of co-localization between RNA detected with acridine orange (red) and DDX1 granules (green). (B) 2-cell stage embryos were treated with 150 μg/ml RNase A, then immunostained with anti-DDX1 antibody. Fewer DDX1 granules were observed after RNase A treatment. In contrast, the distribution of TIA-1 was not substantially different in control versus RNase A-treated embryos. Embryos are displayed as 2D projections of Z-stacks imaged by confocal microscopy. Scale bar = 20 μm.

*Ago2* and *Tif1α* results in embryonic lethality at the 1 to 2 cell stages (Lykke-Andersen et al., 2008; Stein et al., 2015; Torres-Padilla and Zernicka-Goetz, 2006; Wu et al., 2003).

Analysis of DDX1-bound RNAs in 2-cell embryos reveal preferential binding of DDX1 to *Tle6*, *Floped* and *Tif1α*, and likely *Ago2* and *Zar1*. These maternal mRNAs have all been shown to play essential roles in early embryonic development. AGO2 is required for degradation of maternal RNAs prior to transcriptional activation of the zygotic genome. TIF1α has been identified as one of a few factors responsible for activating zygotic genes (Torres-Padilla and Zernicka-Goetz, 2006). FLOPED and TLE6 are two of the four proteins found in the subcortical maternal complex (SCMC) (Li et al., 2008a). The SCMC is essential for embryonic development beyond the 2-cell stage. In mice, ZAR1 is known to be critical for pronuclear syngamy of the embryo (Wu et al., 2003). In *Xenopus*, Zar1 regulates the translation of mRNAs involved in the cell cycle of oocytes (Yamamoto et al., 2013). We propose that spatial-temporal dysregulation of these maternal mRNAs resulting from loss of DDX1 underlies embryonic stalling at the 2- to 4-cell stages.

In summary, we show that DDX1 is an essential protein in embryonic development, with DDX1 knockout causing embryos to stall at the 2- to 4-cell stages. DDX1 forms large granules in the cytoplasm of early-stage embryos, with stress granule markers TIA-1 and TIAR co-localizing with DDX1 in these granules. RNA is required for retention of DDX1, but not TIA-1, in these granules. RNA-DDX1 immunoprecipitation analysis indicates that DDX1 binds to maternal RNAs previously shown to play key roles in embryonic development beyond the 2-cell stage. We postulate that DDX1 plays a critical role in the temporal-spatial protection of maternal RNAs required for early embryonic development.

#### 4. Materials and methods

##### 4.1. Embryo and oocyte collection

The generation of a *Ddx1* knockout line has been described previously (Hildebrandt et al., 2015). Naturally mated heterozygote *Ddx1*<sup>+/−</sup> and C57BL/6 or FVB mice were checked for the presence of a vaginal plug, with plug date designated as embryonic day (E) 0.5. For collection of E0.5 to E2.5 embryos, the oviducts and uterus were removed and placed

in prewarmed (37 °C) M2 flush medium (Sigma-Aldrich). Oviducts were flushed using a capillary tube to collect E0.5 to E2.5 embryos. The uterine horns were flushed to collect E3.5 embryos. E0.5 single cell embryos were treated with 300 μg/ml hyaluronidase (Sigma-Aldrich) for 30 s to 1 min to remove the cumulus cells.

To obtain germinal vesical (GV) stage oocytes, ovaries were dissected from adult female mice. Ovaries were placed in prewarmed (37 °C) M2 medium. The ovaries were poked extensively with a fine needle under a dissecting microscope to release oocytes. Cumulus cells were removed with hyaluronidase as described above. For immunostaining, oocytes were placed in PBS and processed as described below for preimplantation embryos. For *in vitro* maturation to meiosis I (MI) (Kidder, 2014), oocytes were allowed to mature to meiosis I (MI) by culturing in previously prepared drops of KSOM medium under oil for 24–48 h at 37 °C in 5% CO<sub>2</sub>. To obtain MII-arrested oocytes, FVB/N wild-type females were injected with 5 IU pregnant mare serum gonadotropin (Intervet) followed by 5 IU chorionic gonadotropin (Intervet) approximately 46 h later (Luo et al., 2011). Females were euthanized by cervical dislocation. The oviducts were flushed using a capillary tube to release the oocytes into M2 medium (Sigma-Aldrich) containing 300 μg/ml hyaluronidase to remove the cumulus cells. Oocytes were then rinsed in M2 medium and immunostained as described below for embryos.

##### 4.2. Culturing pre-implantation embryos and hatching blastocysts

At least 30 min before collecting embryos, M16 or KSOM medium (Sigma-Aldrich) was prepared by placing 25 μl drops covered with embryo-tested mineral oil (Sigma-Aldrich) in a 24-well dish. Three larger (100 μl) drops of medium covered with mineral oil were also prepared for washing the embryos following flushing. The dish was placed in a 5% CO<sub>2</sub> incubator for equilibration. Embryos were collected, rinsed 3X in M16 medium, placed in the 25 μl M16 or KSOM droplets and cultured for the designated times.

For hatching blastocysts, embryos were cultured in high glucose DMEM supplemented with 15% FCS, 0.1 mM β-mercaptoethanol (β-ME), 1X sodium pyruvate (Gibco), 1X non-essential amino acids (Gibco) and penicillin and streptomycin on gelatin-coated wells or coverslips.

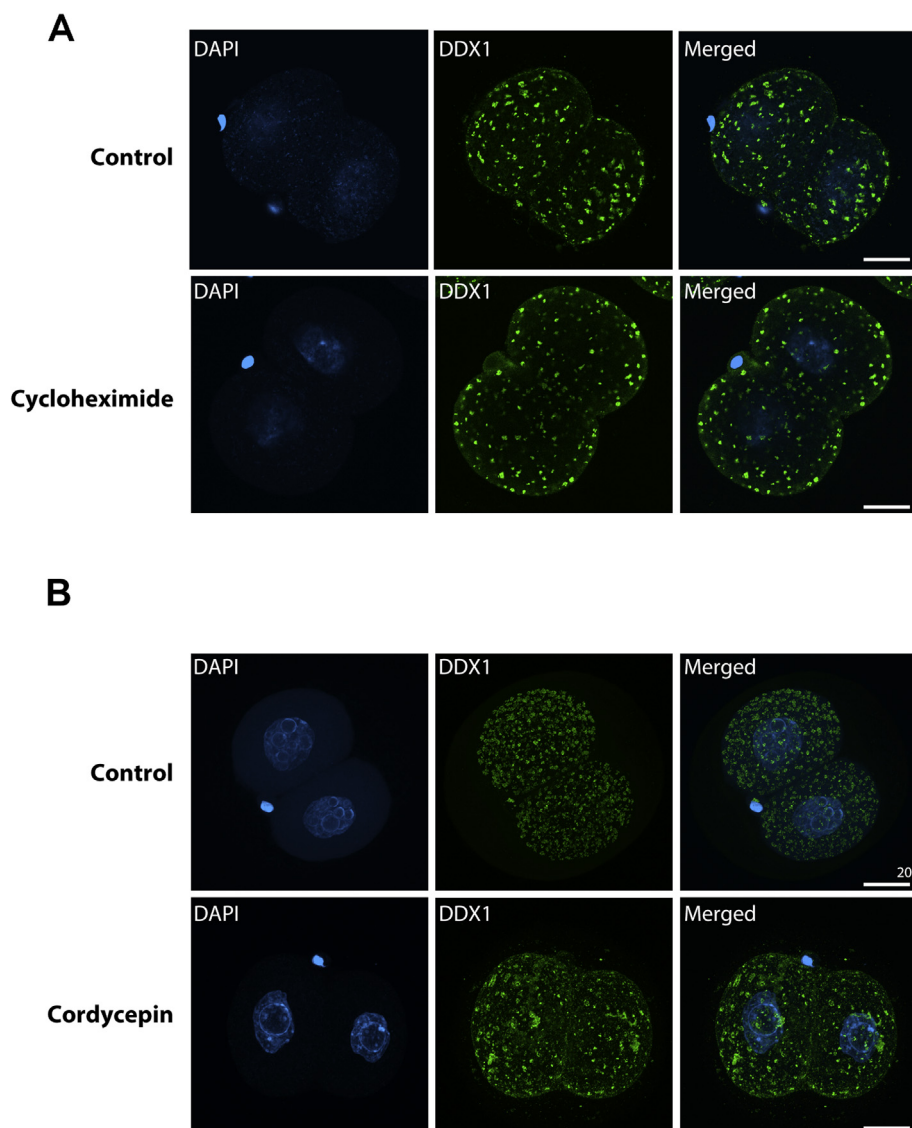


**Fig. 9. Effects of transcription or translation inhibition on DDX1 granules in E1.5 embryos.** (A) 2-cell embryos were treated with either 150 µg/ml cycloheximide (inhibition of translation) or (B) 200 µM cordycepin (inhibition of transcription) for 8 h. Untreated 2-cell stage embryos were used as control. The numbers and appearance of DDX1 granules were affected by inhibition of transcription but not inhibition of translation. Embryos are displayed as 2D projections of Z-stacks imaged by confocal microscopy. Scale bar = 20 µm.

**Table 1**

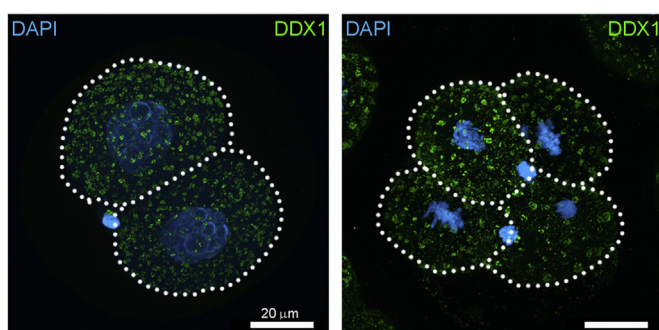
Stalling of embryos generated from heterozygous intercrosses prior to blastocyst stage.

Starting material		24 h	48 h	72 h
E0.5 embryos				
Wild-type intercrosses (2 crosses)	1-cell	2 (12%)	1 (5%)	1 (5%)
	2-cell	15 (88%)	0	0
	4-cell	–	16 (94%)	0
	8-cell	–	–	16 (94%)
	Total embryos	17	17	17
Heterozygote intercrosses (17 crosses)	1-cell	12 (8%)	12 (8%)	12 (8%)
	2-cell	134 (92%)	35 (24%)	24 (16%)
	4-cell	–	99 (68%)	16 (11%)
	8-cell	–	–	94 (64%)
	Total embryos	146	146	146

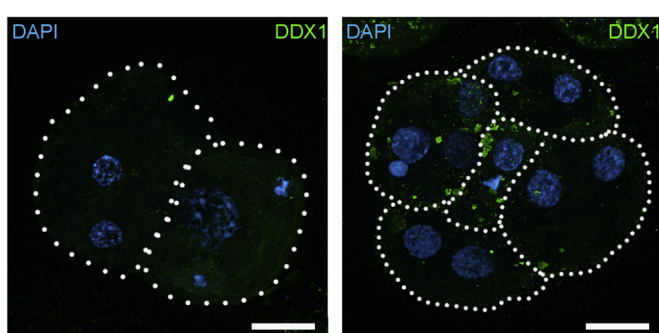
#### 4.3. Immunostaining embryos

Embryos were transferred from flush medium to PBS and washed 2X in PBS. Embryos were fixed in 4% paraformaldehyde for 15 min. The embryos were then washed 3X in PBS + 0.01% Triton-X-100 (PBST), followed by permeabilization in PBS + 0.5% Triton-X-100 for 10 min. The embryos were washed 3X in PBST and incubated in primary antibody containing PBST for a minimum of 1 h at room temperature. Following primary antibody incubation, embryos were washed 3X in PBST and transferred to secondary antibody containing PBST for 1 h at room temperature. The plate was wrapped with foil to minimize exposure to light. After washing 3X in PBST, embryos were placed on a slide and mounted in Mowiol (Calbiochem) containing 1 µg/ml 4',6-diamidino-2-phenylindole (DAPI) to stain the DNA. The primary and secondary antibodies used for immunostaining are listed in Table 2. Anti-DDX1 (2910) was used for all embryo immunostaining. For mitochondria staining, embryos were transferred to M16 droplets containing 100 µM Mito-Tracker Deep Red (Cell Signaling Technology) and incubated at 37 °C for 30 min. Embryos were then fixed and permeabilized in methanol:acetone (1:1 ratio) at 4 °C for 5 min and rehydrated for 30 min with PBST. DDX1 immunostaining after permeabilization in methanol:acetone was as described above.

Embryos were imaged by confocal microscopy using a Zeiss LSM710

**A** 2-cell

## 4-cell

**B** Stalled 2-cell

## Stalled 4-cell

**Fig. 10.** Embryos from *Ddx1*<sup>+/−</sup> intercrosses stall at the 2- to 4-cell stages. (A) Wild-type embryos were collected and immunostained with anti-DDX1 antibody. Nuclei were visualized with DAPI. (B) Embryos from first generation heterozygote intercrosses were collected at E0.5 and cultured at 37 °C for 72 h. After 72 h, embryos should be at the 8–16 cell stages. Instead, some of the embryos were stalled at the 2- and 4-cell stages. DDX1 immunostaining of these stalled embryos revealed significantly reduced DDX1 levels throughout the cytoplasm. Embryos are displayed as 2D projections of Z-stacks imaged by confocal microscopy. Scale bar = 20 μm.

**Table 2**

Antibodies used for immunohistochemistry and immunofluorescence.

Antibody	Host	Dilution	Source
anti-DDX1 (2910)	Rabbit	1:800	In house (batch 2910) ( <a href="#">Bleoo et al., 2001</a> )
anti-DDX1 (2290)	Rabbit	1:500	In house (batch 2290)
anti-CstF64	Mouse	1:100	Dr. James Manley, Columbia University
anti-SMN	Mouse	1:1000	ImmunoQuest, Cat. # IQ202
anti-DDX3	Mouse	1:200	Santa Cruz, Cat. # sc-81247
anti-EXOSC5	Mouse	1:100	Abcam, Cat. # ab69699
anti-GW182	Mouse	1:50	Dr. Marvin Fritzler, University of Calgary
anti-RACK1	Mouse	1:400	Transduction Laboratories, Cat. #R20620
anti-FXR1	Goat	1:100	Santa Cruz, Cat. # sc-10554
anti-TIAR	Goat	1:400	Santa Cruz, Cat. # sc-1749
anti-TIA-1	Goat	1:400	Santa Cruz, Cat. # sc-1751
anti-DDX6	Mouse	1:300	Abnova, Cat. #H00001656-M01
anti-Calnexin	Mouse	1:200	Santa Cruz, Cat. # sc-6465
anti-Rabbit Alexa-488	Donkey	1:400	Molecular Probes, ThermoFisher
anti-Goat Alexa-488	Donkey	1:400	Molecular Probes, ThermoFisher
anti-Mouse Alexa-555	Donkey	1:400	Molecular Probes, ThermoFisher
anti-Goat Alexa-555	Donkey	1:400	Molecular Probes, ThermoFisher
anti-Rabbit Alexa-555	Donkey	1:400	Molecular Probes, ThermoFisher

laser scanning microscope and a plan-apochromat 40X/1.4 lens to capture single sections. Z-stacks were taken at 0.35 μm intervals. Cytoplasmic DDX1 granules were analysed with Imaris software v7.0 (Bitplane). All images were processed with a 3 × 3 × 1 median filter followed by surface analysis. Surfaces were not smoothed and an absolute threshold of 200 voxels (3D pixels) was used to define surfaces. A minimum threshold of 200 voxels was used to define the minimum aggregate size. Six to ten embryos were analysed for each developmental stage and the volumes of the DDX1 granules were compared using a box and whisker plot (Prism). Statistical analysis was by one-way ANOVA.

**4.4. Acridine orange staining embryos and RNase a treatment**

Acridine orange (2 μM; Sigma-Aldrich) was used to stain RNA in embryos. For RNase treatment, embryos were collected and transferred to warm DMEM +5 mM HEPES (pH 7.5) in a 24 well dish. The embryos were transferred to PBS +0.1% saponin for 6 min at room temperature then incubated in PBS containing 150 μg/ml RNase A for 30 min at 37 °C. Embryos were then washed in PBS twice before immunofluorescence staining. This method was adapted from [Li et al. \(2008b\)](#).

**4.5. Transcription and translation inhibition**

M16 medium (25 μl) containing either 200 μM cordycepin (Sigma-Aldrich) or 150 μg/ml cycloheximide (Sigma-Aldrich) was used for transcription or translation inhibition, respectively. Untreated 2-cell stage embryos served as controls. M16 medium droplets were covered with mineral oil and incubated at 37 °C at least 30 min before the transfer of embryos. E1.5 embryos were collected from flush medium and washed 3X in M16 medium before transferring to the 25 μl M16 medium droplets.

**4.6. Immunohistochemistry**

OCT and paraffin-embedded tissues were sectioned. OCT-embedded tissue sections were processed for antigen retrieval by heating tissue sections covered with 10 mM citrate buffer containing 0.05% Tween-20 at pH 6.0–100 °C, followed by microwaving at 750 W for 6 min. For

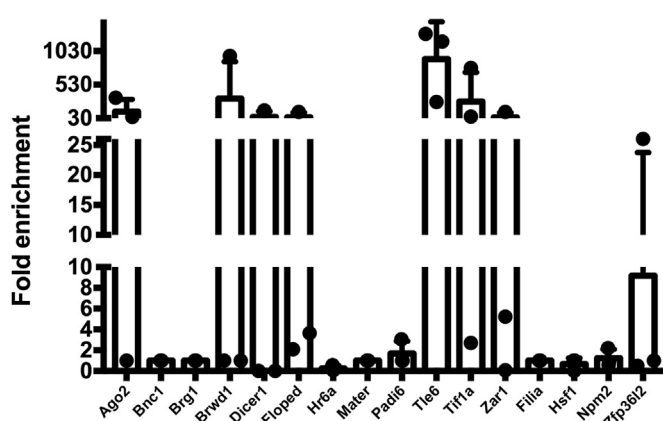


**Fig. 11.** DDX1-bound RNAs in 2-cell mouse embryos. DDX1 with its bound RNAs was immunoprecipitated from 2-cell stage embryos using anti-DDX1 antibody (or IgG as control). RT-qPCR analysis was carried out using primers to 16 genes essential for mouse embryo development. Pre-amplifications (n = 3) were carried out to generate sufficient cDNA for analysis. The average fold enrichment (anti-DDX1 antibody over IgG) in 3 pre-amplification reactions is shown for each gene.

paraffin-embedded tissue sections, tissues were first de-waxed by dipping in xylene 3X for 10 min each. Tissue sections were then hydrated through a series of ethanol, from 100% ethanol to ddH<sub>2</sub>O and TBS. Antigen retrieval was as described above and the slides washed with TBST (0.05% Tween 20) for 5 min. From this point, OCT- and paraffin-embedded tissue sections were treated the same. Tissue sections were blocked for 30 min to 1 h in 0.5% fish gelatin in TBST (0.1% Tween 20), followed by an overnight incubation at 4 °C with primary antibody diluted in Dako Antibody Diluent. After a series of washes in TBS and TBST (0.05% Tween 20), background peroxidase activity was removed by incubating slides in 3% H<sub>2</sub>O<sub>2</sub> in TBS for 15 min. Dakocytomation Envision + System Labelled Polymer HRP secondary antibody was added for 1–2 h. Tissue sections were washed in TBST and DAB chromagen in TBS added, followed by DAKO Liquid DAB + Substrate Chromagen System. The DAB signal was darkened by incubating the slides in 1% copper (II) sulphate. For counterstaining, slides were incubated in hematoxylin for 1–5 min, washed, and incubated in saturated lithium carbonate for ~2 min (to obtain a light blue color). Slides were coverslipped with VectaMount AG (Vector Laboratories). Images were captured with an Axioskop 2 Plus microscope with Zeiss 10X/0.3, 20X/0.75 and 40X/1.3 lenses.

#### 4.7. RNA isolation and RT-PCR

Total RNA from adult mouse brain tissue was isolated using the TRIzol reagent (Thermo Fisher Scientific). Total RNAs were extracted from either seven (mouse 1) or eight (mouse 2) 2-cell embryos using the RNeasy Plus Micro Kit (Qiagen) following the manufacturer's protocol. RNAs were reverse transcribed using SuperScript IV (Invitrogen) and oligo(dT). PCR reactions were carried out using the following primers and conditions. For exons 1 to 9 amplification, nested PCR was carried out using forward primer 5'-CCCGCAGCGGAGGAGTG-3' and reverse primer 5'-TAATTATCAAATTGTTTATTATGAGA-3' for the first round of PCR, and forward primer 5'-AAGATGGCGGCCTCTCC-3' and reverse primer 5'-TAATTATCAAATTGTTTATTATGAGA-3' for nested PCR. For exons 10 to 16 amplification, we used forward primer 5'-AATTCACTATGCATGATAC-3' and reverse primer 5'-AACTCTTTCCCACACGT-3'. For exons 17 to 21, we used forward primer 5'-TGATTGTTGCTCTGC-TACTC-3' and reverse primer 5'-CATAAGGAACGCCATGGATAT-3'. For exons 22 to 26, we used forward primer 5'-ACCCTGCCTGATGAGAAC-3' and reverse primer 5'-TATAGITGTCAAGTTATTCATT-3'. All PCR reactions (including nested PCRs) were performed under the following conditions: pre-PCR (94 °C 5 min), 40 cycles (94 °C 30 s, 58 °C 30 s, 72 °C 30 s) with a final extension (72 °C 7 min).

#### 4.8. Western blotting

Whole cell lysates were prepared from two hundred 2-cell embryos, mouse R1 embryonic stem cells and adult mouse brain tissue. Embryos were first treated with Acidic Tyrode's solution (Sigma) to dissolve the zona pellucida. They were then washed with 2X PBS and frozen in liquid nitrogen. Embryos, R1 cells and brain tissue were lysed in lysis buffer [50 mM Tris-HCl pH 7.5, 150 mM NaCl, 1% sodium deoxycholate, 1% Triton-X-100, 1 mM EDTA, 0.1% SDS, 1 mM DTT, 1X PhosStop (Roche) phosphatase inhibitors and 1X Complete (Roche) protease inhibitors]. The entire 2-cell embryo lysate was mixed with loading buffer, boiled and loaded onto a SDS-PAGE gel. For R1 cells, we loaded 2.5, 5, 10 µg of lysate. For comparison of R1 cells and brain tissue, 40 µg of proteins was loaded in each lane. Proteins were transferred to a PVDF membrane and immunoblotted with two different anti-DDX1 antibodies: anti-DDX1 (2910), targeting aa 1–186, and anti-DDX1 (2290), targeting aa 187–740. R1 and mouse brain blots were also immunoblotted with anti-actin antibody.

#### 4.9. RNA immunoprecipitation, pre-amplification and RT-qPCR

Embryos were collected in PBS and frozen in liquid N<sub>2</sub> before storing

at –80 °C. Three hundred embryos were pooled together and divided into 2 groups (IgG, DDX1). 150 embryos per group were lysed in lysis buffer [50 mM Tris-HCl, pH 7.5, 150 mM NaCl, 1% NP-40, 0.5% deoxycholate, 5 mM EDTA, 2 mM DTT, 1X Complete protease inhibitor (Roche) and 200 unit/ml RNase inhibitor (Invitrogen)]. Lysates were pre-cleared with Protein A beads (GE Healthcare), followed by incubation with either IgG-purified rabbit-anti-DDX1 antibody or pre-immune serum at 4 °C for 90 min with rotation. Protein A beads were then added and samples were incubated for another 45 min. Immunoprecipitates were washed 5 times in wash buffer [50 mM Tris-HCl, pH 7.5, 1 M NaCl, 1% NP-40, 1% deoxycholate and 5 mM EDTA], followed by one wash in 1X RQ1 DNase buffer (40 mM Tris-HCl, pH 8.0, 10 mM MgSO<sub>4</sub>, 1 mM CaCl<sub>2</sub>). Immunoprecipitates were digested with 8 unit/ml of RQ1 DNase (Promega) at 37 °C for 30 min, followed by digestion with 250 µg/ml of Proteinase K (Roche) at 37 °C for 30 min. Co-immunoprecipitated RNAs were extracted with sodium acetate (pH 5.2)-equilibrated phenol (Roche) and precipitated with ethanol. Precipitated RNAs were resuspended in H<sub>2</sub>O and reverse-transcribed to cDNA using random hexamers and Superscript IV reverse transcriptase (Invitrogen) following the manufacturer's instructions. cDNAs were then pre-amplified using 16 different primer sets (Table 3) at a final concentration of 36 nM for each primer. The pre-amplification PCR reaction was using Phusion DNA polymerase (NEB) at 60 °C and 14 cycles of PCR amplification. The pre-amplification steps were adapted and modified from (Andersson et al., 2015) and the protocol of Cell-to-CT kits (Thermo Fisher Scientific). The cDNA products were then diluted 8-fold with nuclease-free water. For RT-qPCR, 1 µl of diluted cDNA was used for each 10 µl reaction containing BrightGreen 2X-qPCR MasterMix-ROX (Applied Biological Materials). PCR was performed in 96-well plates using the QuantStudio 6 Flex Real-Time PCR system (Applied Biosystems). The run method was customized as follows: Pre-PCR (Ramp rate 1.9 °C/s, 95 °C for 10 min), 40 cycles PCR (Ramp rate 1.9 °C/s, 95 °C 15 s, Ramp rate 1.9 °C/s, 58 °C 30 s, Ramp rate 1.6 °C/s, 72 °C 1 min). Results were exported in Excel, and analysed with Prism. Ct values above 36 were considered as 36.

**Table 3**  
Primers used for RT-qPCR.

Zar1 Fwd	CGATGGGTTCTGTCAAC
Zar1 Rev	GAGAGGCCACAGAACGGTCA
Ago2 Fwd	AGAATAACGGGCTGTGGTGTAT
Ago2 Rev	GAAGCAGGTACAAGAACGG
Tif1α Fwd	TGCTCTGAGGAAACCGTGT
Tif1α Rev	CATGCACAGGGGACTCTG
Dicer1 Fwd	TIGCCTGCATTTCCGTTG
Dicer1 Rev	AAGCTCTCTGTGTGTCGG
Brwd1 Fwd	TGCACTGGAAAGCTGTGTA
Brwd1 Rev	AGGACCCATCAACGACATGG
Hr6a Fwd	CCATCTAACGCTATGGCAG
Hr6a Rev	CCGCTTGTCTCTGGTAC
Brg1 Fwd	CCAGCGGTATGTCAGTGT
Brg1 Rev	CATACACCTGGCAAGCAA
Bnc1 Fwd	GCAGGATGGCTGAGGCTAT
Bnc1 Rev	TCGAACACCCATGGACTG
Mater Fwd	AGCAGACATCAGATAATGGAG
Mater Rev	GGTGTGAGGCTGAAGGTT
Floped Fwd	GCCTGGCACAAAGAAAACGA
Floped Rev	GCCAGCCAGTTTAGCCCT
Padi6 Fwd	CAACCAGCAGGACCAAC
Padi6 Rev	GGGGCTCCAGTAATCCACA
Tle6 Fwd	GGGGCCTCCAACTCTCA
Tle6 Rev	ATTCAGAGACGACGCTGTCT
Filia Fwd	AGCTTGGCTGAGTAAGGC
Filia Rev	CTCTACTCTGTCTCCCGA
Zfp3612 Fwd	AACGCCACAATTCCGTCCT
Zfp3612 Rev	TTTGCAGGGATTCTCCGT
Npm2 Fwd	GCAGCGCAACACAGTGTATA
Npm2 Rev	TGTTGGGACTCATGTCGATT
Hsf1 Fwd	TGCTGGACATTCAAGGAGCT
Hsf1 Rev	CTCCCTGTGTCCACAGCAT

## Competing interests

The authors declare that they have no competing interests.

## Acknowledgments

We are grateful to Kacie Norton and Dr. Heather McDermid for their help with dissections and superovulation. We thank Dr. James Manley, Columbia University, for the anti-CstF64 antibody and Dr. Marvin Fritzler, University of Calgary, for the anti-GW182 antibody. This work was supported by grants from the Canadian Institutes of Health Research - grant number 162157.

## Appendix A. Supplementary data

Supplementary data to this article can be found online at <https://doi.org/10.1016/j.ydbio.2019.07.014>.

## References

- Akiyama, K., Akao, Y., Yokoyama, M., Nakagawa, Y., Noguchi, T., Yagi, K., Nishi, Y., 1999. Expression of two dead box genes (DDX1 and DDX6) is independent of that of MYCN in human neuroblastoma cell lines. *Biochem. Mol. Biol. Int.* 47, 563–568.
- Amler, L.C., Schurmann, J., Schwab, M., 1996. The DDX1 gene maps within 400 kbp 5' to MYCN and is frequently coamplified in human neuroblastoma. *Genes Chromosomes Cancer* 15, 134–137.
- Anderson, P., Kedersha, N., 2008. Stress granules: the Tao of RNA triage. *Trends Biochem. Sci.* 33, 141–150.
- Andersson, D., Akrap, N., Svec, D., Godfrey, T.E., Kubista, M., Landberg, G., Stahlberg, A., 2015. Properties of targeted preamplification in DNA and cDNA quantification. *Expert Rev. Mol. Diagn.* 15, 1085–1100.
- Arimoto-Matsuzaki, K., Saito, H., Takekawa, M., 2016. TIA1 oxidation inhibits stress granule assembly and sensitizes cells to stress-induced apoptosis. *Nat. Commun.* 7, 10252.
- Arimoto, K., Fukuda, H., Imajoh-Ohmi, S., Saito, H., Takekawa, M., 2008. Formation of stress granules inhibits apoptosis by suppressing stress-responsive MAPK pathways. *Nat. Cell Biol.* 10, 1324–1332.
- Ayache, J., Benard, M., Ernoult-Lange, M., Minshall, N., Standart, N., Kress, M., Weil, D., 2015. P-body assembly requires DDX6 repression complexes rather than decay or Ataxin2/2L complexes. *Mol. Biol. Cell* 26, 2579–2595.
- Balko, J.M., Arteaga, C.L., 2011. Dead-box or black-box: is DDX1 a potential biomarker in breast cancer? *Breast Canc. Res. Treat.* 127, 65–67.
- Beck, A.R., Miller, I.J., Anderson, P., Streuli, M., 1998. RNA-binding protein TIAR is essential for primordial germ cell development. *Proc. Natl. Acad. Sci. U. S. A.* 95, 2331–2336.
- Biase, F.H., Cao, X., Zhong, S., 2014. Cell fate inclination within 2-cell and 4-cell mouse embryos revealed by single-cell RNA sequencing. *Genome Res.* 24, 1787–1796.
- Bierkamp, C., Luxey, M., Metchat, A., Audouard, C., Dumollard, R., Christians, E., 2010. Lack of maternal Heat Shock Factor 1 results in multiple cellular and developmental defects, including mitochondrial damage and altered redox homeostasis, and leads to reduced survival of mammalian oocytes and embryos. *Dev. Biol.* 339, 338–353.
- Bleoo, S., Sun, X., Hendzel, M.J., Rowe, J.M., Packer, M., Godbout, R., 2001. Association of human DEAD box protein DDX1 with a cleavage stimulation factor involved in 3'-end processing of pre-mRNA. *Mol. Biol. Cell* 12, 3046–3059.
- Bley, N., Lederer, M., Pfalz, B., Reinke, C., Fuchs, T., Glass, M., Moller, B., Huttelmaier, S., 2015. Stress granules are dispensable for mRNA stabilization during cellular stress. *Nucleic Acids Res.* 43, e26.
- Carter, M.G., Hamatani, T., Sharov, A.A., Carmack, C.E., Qian, Y., Aiba, K., Ko, N.T., Dudekula, D.B., Brzoska, P.M., Hwang, S.S., Ko, M.S., 2003. In situ-synthesized novel microarray optimized for mouse stem cell and early developmental expression profiling. *Genome Res.* 13, 1011–1021.
- Chahar, H.S., Chen, S., Manjunath, N., 2013. P-body components LSM1, GW182, DDX3, DDX6 and XRN1 are recruited to WNV replication sites and positively regulate viral replication. *Virology* 436, 1–7.
- Chen, H.C., Lin, W.C., Tsay, Y.G., Lee, S.C., Chang, C.J., 2002. An RNA helicase, DDX1, interacting with poly(A) RNA and heterogeneous nuclear ribonucleoprotein K. *J. Biol. Chem.* 277, 40403–40409.
- Christians, E., Davis, A.A., Thomas, S.D., Benjamin, I.J., 2000. Maternal effect of Hsf1 on reproductive success. *Nature* 407, 693–694.
- Chuma, S., Hosokawa, M., Kitamura, K., Kasai, S., Fujioka, M., Hiyoshi, M., Takamune, K., Noce, T., Nakatsuji, N., 2006. Tdrd1/Mtr-1, a tudor-related gene, is essential for male germ-cell differentiation and nuage/germinal granule formation in mice. *Proc. Natl. Acad. Sci. U. S. A.* 103, 15894–15899.
- Clapier, C.R., Cairns, B.R., 2009. The biology of chromatin remodeling complexes. *Annu. Rev. Biochem.* 78, 273–304.
- Clark, J.M., Eddy, E.M., 1975. Fine structural observations on the origin and associations of primordial germ cells of the mouse. *Dev. Biol.* 47, 136–155.
- Clarke, H.J., 2012. Post-transcriptional control of gene expression during mouse oogenesis. *Results Probl. Cell Differ.* 55, 1–21.
- Eckersley-Maslin, M.A., Alda-Catalinas, C., Reik, W., 2018. Dynamics of the epigenetic landscape during the maternal-to-zygotic transition. *Nat. Rev. Mol. Cell Biol.* 19, 436–450.
- Fagerberg, L., Hallstrom, B.M., Oksvold, P., Kampf, C., Djureinovic, D., Odeberg, J., Habuka, M., Tahmasebpoor, S., Danielsson, A., Edlund, K., Asplund, A., Sjostedt, E., Lundberg, E., Szigyarto, C.A., Skogs, M., Takanen, J.O., Berling, H., Tegel, H., Mulder, J., Nilsson, P., Schwenk, J.M., Lindskog, C., Danielsson, F., Mardinoglu, A., Sivertsson, A., von Feilitzen, K., Forsberg, M., Zahlen, M., Olsson, I., Navani, S., Huss, M., Nielsen, J., Ponten, F., Uhlen, M., 2014. Analysis of the human tissue-specific expression by genome-wide integration of transcriptomics and antibody-based proteomics. *Mol. Cell. Proteom.* 13, 397–406.
- Flemr, M., Ma, J., Schultz, R.M., Svoboda, P., 2010. P-body loss is concomitant with formation of a messenger RNA storage domain in mouse oocytes. *Biol. Reprod.* 82, 1008–1017.
- Gareau, C., Houssin, E., Martel, D., Couder, L., Mellouei, S., Huot, M.E., Laprise, P., Mazroui, R., 2013. Characterization of fragile X mental retardation protein recruitment and dynamics in *Drosophila* stress granules. *PLoS One* 8, e55342.
- Germain, D.R., Graham, K., Glubrecht, D.D., Hugh, J.C., Mackey, J.R., Godbout, R., 2011. DEAD box 1: a novel and independent prognostic marker for early recurrence in breast cancer. *Breast Canc. Res. Treat.* 127, 53–63.
- Germain, D.R., Li, L., Hildebrandt, M.R., Simmonds, A.J., Hughes, S.C., Godbout, R., 2015. Loss of the *Drosophila melanogaster* DEAD box protein Ddx1 leads to reduced size and aberrant gametogenesis. *Dev. Biol.* 407, 232–245.
- Gilks, N., Kedersha, N., Ayodele, M., Shen, L., Stoecklin, G., Dember, L.M., Anderson, P., 2004. Stress granule assembly is mediated by prion-like aggregation of TIA-1. *Mol. Biol. Cell* 15, 5383–5398.
- Godbout, R., Li, L., Liu, R.Z., Roy, K., 2007. Role of DEAD box 1 in retinoblastoma and neuroblastoma. *Future Oncol.* 3, 575–587.
- Godbout, R., Packer, M., Bie, W., 1998. Overexpression of a DEAD box protein (DDX1) in neuroblastoma and retinoblastoma cell lines. *J. Biol. Chem.* 273, 21161–21168.
- Godbout, R., Packer, M., Katyal, S., Bleoo, S., 2002. Cloning and expression analysis of the chicken DEAD box gene DDX1. *Biochim. Biophys. Acta* 1574, 63–71.
- Godbout, R., Squire, J., 1993. Amplification of a DEAD box protein gene in retinoblastoma cell lines. *Proc. Natl. Acad. Sci. U. S. A.* 90, 7578–7582.
- Griffin, C.T., Brennan, J., Magnuson, T., 2008. The chromatin-remodeling enzyme BRG1 plays an essential role in primitive erythropoiesis and vascular development. *Development* 135, 493–500.
- Hamatani, T., Carter, M.G., Sharov, A.A., Ko, M.S., 2004. Dynamics of global gene expression changes during mouse preimplantation development. *Dev. Cell* 6, 117–131.
- Han, C., Liu, Y., Wan, G., Choi, H.J., Zhao, L., Ivan, C., He, X., Sood, A.K., Zhang, X., Lu, X., 2014. The RNA-binding protein DDX1 promotes primary microRNA maturation and inhibits ovarian tumor progression. *Cell Rep.* 8, 1447–1460.
- Herman, A.B., Vrakas, C.N., Ray, M., Kelemen, S.E., Sweredoski, M.J., Moradian, A., Haines, D.S., Autieri, M.V., 2018. FXR1 is an IL-19-responsive RNA-binding protein that destabilizes pro-inflammatory transcripts in vascular smooth muscle cells. *Cell Rep.* 24, 1176–1189.
- Hildebrandt, M.R., Germain, D.R., Monckton, E.A., Brun, M., Godbout, R., 2015. Ddx1 knockout results in transgenerational wild-type lethality in mice. *Sci. Rep.* 5, 9829.
- Jiao, Z.X., Woodruff, T.K., 2013. Detection and quantification of maternal-effect gene transcripts in mouse second polar bodies: potential markers of embryo developmental competence. *Fertil. Steril.* 99, 2055–2061.
- Kanai, Y., Dohmae, N., Hirokawa, N., 2004. Kinesin transports RNA: isolation and characterization of an RNA-transporting granule. *Neuron* 43, 513–525.
- Kedersha, N.L., Gupta, M., Li, W., Miller, I., Anderson, P., 1999. RNA-binding proteins TIA-1 and TIAR link the phosphorylation of eIF-2 alpha to the assembly of mammalian stress granules. *J. Cell Biol.* 147, 1431–1442.
- Kidder, B.L., 2014. In vitro maturation and in vitro fertilization of mouse oocytes and preimplantation embryo culture. *Methods Mol. Biol.* 1150, 191–199.
- Kim, B., Cooke, H.J., Rhee, K., 2012. DAZL is essential for stress granule formation implicated in germ cell survival upon heat stress. *Development* 139, 568–578.
- Kim, K.H., Lee, K.A., 2014. Maternal effect genes: findings and effects on mouse embryo development. *Clin Exp Reprod Med* 41, 47–61.
- Kunde, S.A., Musante, L., Grimes, A., Fischer, U., Muller, E., Wanker, E.E., Kalscheuer, V.M., 2011. The X-chromosome-linked intellectual disability protein PQBP1 is a component of neuronal RNA granules and regulates the appearance of stress granules. *Hum. Mol. Genet.* 20, 4916–4931.
- Lai, M.C., Lee, Y.H., Tarn, W.Y., 2008. The DEAD-box RNA helicase DDX3 associates with export messenger ribonucleoproteins as well as tip-associated protein and participates in translational control. *Mol. Biol. Cell* 19, 3847–3858.
- Li, L., Baibakov, B., Dean, J., 2008a. A subcortical maternal complex essential for preimplantation mouse embryogenesis. *Dev. Cell* 15, 416–425.
- Li, L., Germain, D.R., Poon, H.Y., Hildebrandt, M.R., Monckton, E.A., McDonald, D., Hendzel, M.J., Godbout, R., 2016. DEAD box 1 facilitates removal of RNA and homologous recombination at DNA double-strand breaks. *Mol. Cell. Biol.* 36, 2794–2810.
- Li, L., Monckton, E.A., Godbout, R., 2008b. A role for DEAD box 1 at DNA double-strand breaks. *Mol. Cell. Biol.* 28, 6413–6425.
- Li, L., Poon, H.Y., Hildebrandt, M.R., Monckton, E.A., Germain, D.R., Fahlman, R.P., Godbout, R., 2017. Role for RIF1-interacting partner DDX1 in BLM recruitment to DNA double-strand breaks. *DNA Repair (Amst)* 55, 47–63.
- Li, L., Roy, K., Katyal, S., Sun, X., Bleoo, S., Godbout, R., 2006. Dynamic nature of cleavage bodies and their spatial relationship to DDX1 bodies, Cajal bodies, and gems. *Mol. Biol. Cell* 17, 1126–1140.
- Li, L., Zheng, P., Dean, J., 2010. Maternal control of early mouse development. *Development* 137, 859–870.

- Lin, M.H., Sivakumaran, H., Jones, A., Li, D., Harper, C., Wei, T., Jin, H., Rustanti, L., Meunier, F.A., Spann, K., Harrich, D., 2014. A HIV-1 Tat mutant protein disrupts HIV-1 Rev function by targeting the DEAD-box RNA helicase DDX1. *Retrovirology* 11, 121.
- Lue, Y.H., Hikim, A.P., Swerdlow, R.S., Im, P., Taing, K.S., Bui, T., Leung, A., Wang, C., 1999. Single exposure to heat induces stage-specific germ cell apoptosis in rats: role of intratesticular testosterone on stage specificity. *Endocrinology* 140, 1709–1717.
- Luo, C., Zuniga, J., Edison, E., Palla, S., Dong, W., Parker-Thornburg, J., 2011. Superovulation strategies for 6 commonly used mouse strains. *J. Am. Assoc. Lab. Anim. Sci.* 50, 471–478.
- Lykke-Andersen, K., Gilchrist, M.J., Grabarek, J.B., Das, P., Miska, E., Zernicka-Goetz, M., 2008. Maternal Argonaute 2 is essential for early mouse development at the maternal-zygotic transition. *Mol. Biol. Cell* 19, 4383–4392.
- Ma, J., Zeng, F., Schultz, R.M., Tseng, H., 2006. Basonuclin: a novel mammalian maternal-effect gene. *Development* 133, 2053–2062.
- Maekawa, S., Imamachi, N., Irie, T., Tani, H., Matsumoto, K., Mizutani, R., Imamura, K., Kakeda, M., Yada, T., Sugano, S., Suzuki, Y., Akimitsu, N., 2015. Analysis of RNA decay factor mediated RNA stability contributions on RNA abundance. *BMC Genomics* 16, 154.
- Mazroui, R., Huot, M.E., Tremblay, S., Filion, C., Labelle, Y., Khandjian, E.W., 2002. Trapping of messenger RNA by Fragile X Mental Retardation protein into cytoplasmic granules induces translation repression. *Hum. Mol. Genet.* 11, 3007–3017.
- McDonald, K.K., Aulas, A., Destroismaisons, L., Pickles, S., Beleac, E., Camu, W., Rouleau, G.A., Vande Velde, C., 2011. TAR DNA-binding protein 43 (TDP-43) regulates stress granule dynamics via differential regulation of G3BP and TIA-1. *Hum. Mol. Genet.* 20, 1400–1410.
- McLay, D.W., Clarke, H.J., 2003. Remodelling the paternal chromatin at fertilization in mammals. *Reproduction* 125, 625–633.
- Miller, L.C., Blandford, V., McAdam, R., Sanchez-Carbente, M.R., Badeaux, F., DesGroseilliers, L., Sossin, W.S., 2009. Combinations of DEAD box proteins distinguish distinct types of RNA: protein complexes in neurons. *Mol. Cell. Neurosci.* 40, 485–495.
- Murchison, E.P., Stein, P., Xuan, Z., Pan, H., Zhang, M.Q., Schultz, R.M., Hannon, G.J., 2007. Critical roles for Dicer in the female germline. *Genes Dev.* 21, 682–693.
- Noguchi, T., Akiyama, K., Yokoyama, M., Kanda, N., Matsunaga, T., Nishi, Y., 1996. Amplification of a DEAD box gene (DDX1) with the MYCN gene in neuroblastomas as a result of cosegregation of sequences flanking the MYCN locus. *Genes Chromosomes Cancer* 15, 129–133.
- Nothias, J.Y., Majumder, S., Kaneko, K.J., DePamphilis, M.L., 1995. Regulation of gene expression at the beginning of mammalian development. *J. Biol. Chem.* 270, 22077–22080.
- Nothias, J.Y., Miranda, M., DePamphilis, M.L., 1996. Uncoupling of transcription and translation during zygotic gene activation in the mouse. *EMBO J.* 15, 5715–5725.
- Ogushi, S., Yamagata, K., Obuse, C., Furuta, K., Wakayama, T., Matzuk, M.M., Saitou, M., 2017. Reconstitution of the oocyte nucleolus in mice through a single nucleolar protein NPM2. *J. Cell Sci.* 130, 2416–2429.
- Ohn, T., Kedersha, N., Hickman, T., Tisdale, S., Anderson, P., 2008. A functional RNAi screen links O-GlcNAc modification of ribosomal proteins to stress granule and processing body assembly. *Nat. Cell Biol.* 10, 1224–1231.
- Ohsugi, M., Zheng, P., Baibakov, B., Li, L., Dean, J., 2008. Maternally derived FILIA-MATER complex localizes asymmetrically in cleavage-stage mouse embryos. *Development* 135, 259–269.
- Onishi, H., Kino, Y., Morita, T., Futai, E., Sasagawa, N., Ishiura, S., 2008. MBNL1 associates with YB-1 in cytoplasmic stress granules. *J. Neurosci. Res.* 86, 1994–2002.
- Oshikawa, K., Matsumoto, M., Oyamada, K., Nakayama, K.I., 2012. Proteome-wide identification of ubiquitylation sites by conjugation of engineered lysine-less ubiquitin. *J. Proteome Res.* 11, 796–807.
- Pattabiraman, S., Baumann, C., Guisado, D., Eppig, J.J., Schimenti, J.C., De La Fuente, R., 2015. Mouse BRWD1 is critical for spermatid postmeiotic transcription and female meiotic chromosome stability. *J. Cell Biol.* 208, 53–69.
- Pepling, M.E., Wilhelm, J.E., O'Hara, A.L., Gephhardt, G.W., Spradling, A.C., 2007. Mouse oocytes within germ cell cysts and primordial follicles contain a Balbiani body. *Proc. Natl. Acad. Sci. U. S. A.* 104, 187–192.
- Perez-Gonzalez, A., Pazó, A., Navajas, R., Ciordia, S., Rodriguez-Frandsen, A., Nieto, A., 2014. hCLE/C14orf166 associates with DDX1-HSPC117-FAM98B in a novel transcription-dependent shuttling RNA-transporting complex. *PLoS One* 9, e90957.
- Philipps, D.L., Wiggleworth, K., Hartford, S.A., Sun, F., Pattabiraman, S., Schimenti, K., Handel, M., Eppig, J.J., Schimenti, J.C., 2008. The dual bromodomain and WD repeat-containing mouse protein BRWD1 is required for normal spermiogenesis and the oocyte-embryo transition. *Dev. Biol.* 317, 72–82.
- Piecyk, M., Wax, S., Beck, A.R., Kedersha, N., Gupta, M., Maritim, B., Chen, S., Gueydan, C., Kruys, V., Streuli, M., Anderson, P., 2000. TIA-1 is a translational silencer that selectively regulates the expression of TNF-alpha. *EMBO J.* 19, 4154–4163.
- Piko, L., Clegg, K.B., 1982. Quantitative changes in total RNA, total poly(A), and ribosomes in early mouse embryos. *Dev. Biol.* 89, 362–378.
- Popow, J., Jurkin, J., Schleifffer, A., Martinez, J., 2014. Analysis of orthologous groups reveals archease and DDX1 as tRNA splicing factors. *Nature* 511, 104–107.
- Proter, D.S.W., Parker, R., 2016. Principles and properties of stress granules. *Trends Cell Biol.* 26, 668–679.
- Ramos, S.B., Stumpo, D.J., Kennington, E.A., Phillips, R.S., Bock, C.B., Ribeiro-Neto, F., Blackshear, P.J., 2004. The CCCH tandem zinc-finger protein Zfp3612 is crucial for female fertility and early embryonic development. *Development* 131, 4883–4893.
- Ribeiro de Almeida, C., Dhir, S., Dhir, A., Moghaddam, A.E., Sattentau, Q., Meinhart, A., Proudfoot, N.J., 2018. RNA helicase DDX1 converts RNA G-quadruplex structures into R-loops to promote IgH class switch recombination. *Mol. Cell* 70, 650–662.e658.
- Robertson-Anderson, R.M., Wang, J., Edgcomb, S.P., Carmel, A.B., Williamson, J.R., Millar, D.P., 2011. Single-molecule studies reveal that DEAD box protein DDX1 promotes oligomerization of HIV-1 Rev on the Rev response element. *J. Mol. Biol.* 410, 959–971.
- Roest, H.P., Baarends, W.M., de Wit, J., van Klaveren, J.W., Wassenaer, E., Hoogerbrugge, J.W., van Cappellen, W.A., Hoeijmakers, J.H., Grootegoed, J.A., 2004. The ubiquitin-conjugating DNA repair enzyme HR6A is a maternal factor essential for early embryonic development in mice. *Mol. Cell. Biol.* 24, 5485–5495.
- Schultz, R.M., 1993. Regulation of zygotic gene activation in the mouse. *Bioessays* 15, 531–538.
- Schultz, R.M., 2002. The molecular foundations of the maternal to zygotic transition in the preimplantation embryo. *Hum. Reprod. Update* 8, 323–331.
- Serman, A., Le Roy, F., Aigueperse, C., Kress, M., Dautry, F., Weil, D., 2007. GW body disassembly triggered by siRNAs independently of their silencing activity. *Nucleic Acids Res.* 35, 4715–4727.
- Singh, A.P., Foley, J.F., Rubino, M., Boyle, M.C., Tandon, A., Shah, R., Archer, T.K., 2016. Brgl enables rapid growth of the early embryo by suppressing genes that regulate apoptosis and cell growth arrest. *Mol. Cell. Biol.* 36, 1990–2010.
- Soto-Rifo, R., Rubilar, P.S., Limousin, T., de Breyne, S., Decimo, D., Ohlmann, T., 2012. DEAD-box protein DDX3 associates with eIF4F to promote translation of selected mRNAs. *EMBO J.* 31, 3745–3756.
- Spiegelman, M., Bennett, D., 1973. A light- and electron-microscopic study of primordial germ cells in the early mouse embryo. *J. Embryol. Exp. Morphol.* 30, 97–118.
- Squire, J.A., Thorner, P.S., Weitzman, S., Maggi, J.D., Dirks, P., Doyle, J., Hale, M., Godbout, R., 1995. Co-activation of MYCN and a DEAD box gene (DDX1) in primary neuroblastoma. *Oncogen* 10, 1417–1422.
- Stein, P., Rozhkov, N.V., Li, F., Cardenas, F.L., Davydenko, O., Vandivier, L.E., Gregory, B.D., Hannon, G.J., Schultz, R.M., 2015. Essential Role for endogenous siRNAs during meiosis in mouse oocytes. *PLoS Genet.* 11, e1005013.
- Tang, F., Kaneda, M., O'Carroll, D., Hajkova, P., Barton, S.C., Sun, Y.A., Lee, C., Tarakhovsky, A., Lao, K., Surani, M.A., 2007. Maternal microRNAs are essential for mouse zygotic development. *Genes Dev.* 21, 644–648.
- Telford, N.A., Watson, A.J., Schultz, R.A., 1990. Transition from maternal to embryonic control in early mammalian development: a comparison of several species. *Mol. Reprod. Dev.* 26, 90–100.
- Tong, Z.B., Gold, L., Pfeifer, K.E., Dorward, H., Lee, E., Bondy, C.A., Dean, J., Nelson, L.M., 2000. Mater, a maternal effect gene required for early embryonic development in mice. *Nat. Genet.* 26, 267–268.
- Torres-Padilla, M.E., Zernicka-Goetz, M., 2006. Role of TIF1alpha as a modulator of embryonic transcription in the mouse zygote. *J. Cell Biol.* 174, 329–338.
- Tritschler, F., Braun, J.E., Eulalio, A., Truffault, V., Izaurralde, E., Weichenrieder, O., 2009. Structural basis for the mutually exclusive anchoring of P body components EDC3 and Tral to the DEAD box protein DDX6/Me31B. *Mol. Cell* 33, 661–668.
- Voronina, E., Seydoux, G., Sassone-Corsi, P., Nagamori, I., 2011. RNA granules in germ cells. *Cold Spring Harb Perspect Biol* 3.
- Wang, Q.T., Piotrowska, K., Cierny, M.A., Milenkovic, L., Scott, M.P., Davis, R.W., Zernicka-Goetz, M., 2004. A genome-wide study of gene activity reveals developmental signaling pathways in the preimplantation mouse embryo. *Dev. Cell* 6, 133–144.
- Wu, X., Viveiros, M.M., Eppig, J.J., Bai, Y., Fitzpatrick, S.L., Matzuk, M.M., 2003. Zygote arrest 1 (Zar1) is a novel maternal-effect gene critical for the oocyte-to-embryo transition. *Nat. Genet.* 33, 187–191.
- Xie, F., Timme, K.A., Wood, J.R., 2018. Using single molecule mRNA fluorescent in situ hybridization (RNA-FISH) to quantify mRNAs in individual murine oocytes and embryos. *Sci. Rep.* 8, 7930.
- Xu, Y., Shi, Y., Fu, J., Yu, M., Feng, R., Sang, Q., Liang, B., Chen, B., Qu, R., Li, B., Yan, Z., Mao, X., Kuang, Y., Jin, L., He, L., Sun, X., Wang, L., 2016. Mutations in PADI6 cause female infertility characterized by early embryonic arrest. *Am. J. Hum. Genet.* 99, 744–752.
- Yamamoto, T.M., Cook, J.M., Kotter, C.V., Khat, T., Silva, K.D., Ferreyros, M., Holt, J.W., Knight, J.D., Charlesworth, A., 2013. Zar1 represses translation in Xenopus oocytes and binds to the TCS in maternal mRNAs with different characteristics than Zar2. *Biochim. Biophys. Acta* 1829, 1034–1046.
- Yurttas, P., Vitale, A.M., Fitzhenry, R.J., Cohen-Gould, L., Wu, W., Gossen, J.A., Coonrod, S.A., 2008. Role for PADI6 and the cytoplasmic lattices in ribosomal storage in oocytes and translational control in the early mouse embryo. *Development* 135, 2627–2636.
- Zeng, F., Schultz, R.M., 2005. RNA transcript profiling during zygotic gene activation in the preimplantation mouse embryo. *Dev. Biol.* 283, 40–57.
- Zinder, J.C., Lima, C.D., 2017. Targeting RNA for processing or destruction by the eukaryotic RNA exosome and its cofactors. *Genes Dev.* 31, 88–100.